

SEGREGATED NETWORK POLYMER-CARBON NANOTUBES
COMPOSITES FOR THERMOELECTRICS

A Thesis

by

DASAROYONG KIM

Submitted to the Office of Graduate Studies of
Texas A&M University
in partial fulfillment of the requirements for the degree of

MASTER OF SCIENCE

August 2009

Major Subject: Mechanical Engineering

SEGREGATED NETWORK POLYMER-CARBON NANOTUBES
COMPOSITES FOR THERMOELECTRICS

A Thesis

by

DASAROYONG KIM

Submitted to the Office of Graduate Studies of
Texas A&M University
in partial fulfillment of the requirements for the degree of

MASTER OF SCIENCE

Approved by:

Chair of Committee,	Choongho Yu
Committee Members,	Jaime C. Grunlan
	Tahir Cagin
Head of Department,	Dennis O'Neal

August 2009

Major Subject: Mechanical Engineering

ABSTRACT

Segregated Network Polymer-Carbon Nanotubes Composites For Thermoelectrics.

(August 2009)

Dasaroyong Kim, B.S., Korea Military Academy

Chair of Advisory Committee: Dr. Choongho Yu

Polymers are intrinsically poor thermal conductors, which are ideal for thermoelectrics, but low electrical conductivity and thermopower have excluded them as feasible candidates as thermoelectric materials in the past. However, recent progress in polymer technology, particularly nanomaterial-polymer composites, can bring them into degenerate semiconductor or metallic regimes by incorporating a small amount of conductive filler. I demonstrate that such polymer nanocomposites can be viable for light-weight and economical thermoelectrics by using a segregated network approach for the nanocomposite synthesis. The thermoelectric properties were further improved by a change of stabilizer and drying conditions. The thermoelectric properties of the segregated network nanocomposites were measured for carbon nanotubes and the thermoelectric figure of merit, ZT , was calculated at room temperature. The influence on thermoelectric properties from filler concentration, stabilizer materials and drying condition are also discussed.

DEDICATION

To my God, my lovely wife Jun Hui and son Allen, who have always been there for me, who love me, and who give their priceless support and encouragement to me.

ACKNOWLEDGMENTS

I am greatly indebted to my advisor Dr. Choongho Yu for his valuable comments and advice. Without his help, this thesis would not have been completed. Sincere thanks to Dr. Jaime C. Grunlan and Dr. Tahir Cagin for their valuable recommendations and consideration as committee members.

TABLE OF CONTENTS

	Page
ABSTRACT.....	iii
DEDICATION.....	iv
ACKNOWLEDGMENTS.....	v
TABLE OF CONTENTS.....	vi
LIST OF FIGURES.....	vii
NOMENCLATURE	x
CHAPTER I INTRODUCTION.....	1
1.1 Literature Review.....	2
1.2 Research Objective.....	7
CHAPTER II EXPERIMENTAL PROCEDURE.....	9
2.1 Composite Materials	10
2.1.1 CNTs Filled with Vinac Emulsion (Stabilizer: Gum Arabic)...	10
2.1.2 CNTs Filled with Airflex Emulsion (Stabilizer: PEDOT:PSS)10	10
2.2 Composite Formation.....	11
2.3 Composite Characterization.....	13
2.3.1 Electrical Conductivity and Thermopower	14
2.3.2 Thermal Conductivity.....	16
CHAPTER III RESULTS AND DISCUSSION	18
3.1 CNTs Filled with Vinac Emulsion (Stabilizer: GA)	18
3.2 CNTs Filled with Airflex Emulsion (Stabilizer: PEDOT:PSS).....	26
CHAPTER IV CONCLUSION.....	39
REFERENCES.....	41
VITA.....	46

LIST OF FIGURES

	Page
Figure 1.1 Crude oil price change trends from May 08 ~ May 09.....	1
Figure 1.2 Diagram of thermoelectric energy conversion with waste heat	3
Figure 1.3 Relationship between thermoelectric properties and their dependence on carrier concentration	4
Figure 1.4 Relationship between thermoelectric properties of segregated network polymer composites and their dependence on carrier concentration.....	6
Figure 2.1 Microstructure of segregated network polymer-CNTs nanocomposite.	9
Figure 2.2 Synthesis of composites in emulsion matrix	12
Figure 2.3 Sample preparation for thermoelectric properties measurement.....	14
Figure 2.4 Experimental equipment for thermoelectric properties measurement	14
Figure 2.5 Home-made shielded box and scheme for thermopower measurement	15
Figure 2.6 Schematic diagram of the setup to measure thermal conductivity	17
Figure 2.7 Experimental setup. Stainless steel rod and thermocouples	17
Figure 3.1 SEM images of 5 (a), 5 (b), 10(c) and 20(d) wt% of CNTs	18
Figure 3.2 Electrical conductivities and thermopower of CNTs filled with vinac emulsion(Stabilizer: GA). The inset is a linear-log plot of the electrical conductivity as a function of the CNT wt %.....	20
Figure 3.3 Thermal conductivities CNTs filled with vinac emulsion (Stabilizer: GA)	21
Figure 3.4 SEM images of 10 wt% of CNTs with 10:1 (a), 3:1 (b), 1:1 (c) and 1:3 (d) with CNTs:GA ratio	21
Figure 3.5 Electrical conductivity of 10 and 3 wt% nanotube-filled composites with different CNTs:GA ratio.....	23

	Page
Figure 3.6 Thermopower of 10 and 3 wt% nanotube-filled composites with different CNTs:GA ratio	23
Figure 3.7 Thermal conductivity of 10 and 3 wt% nanotube-filled composites with different CNTs:GA ratio	24
Figure 3.8 Calculated ZT of 10 and 3 wt% nanotube-filled composites with different CNTs:GA ratio	25
Figure 3.9 Schematic of function of Gum Arabic (a) and PEDOT:PSS (b) and dispersed by PEDOT:PSS in aqueous emulsion as stabilizer (c).....	26
Figure 3.10 SEM cross-section of a 4.4 wt% CNT composite after the composite was freeze-fractured. SEMs of the cross-sections of 6.9, 12.5 and 15 wt% CNT composites are shown in (b), (c) and (d). The ratio between CNT and PEDOT is 1 to 4.....	28
Figure 3.11 SEM of composites dried at room temperature with 1:2(a) and 1:4(c) ratio of CNTs:PEDOT. Composites dried at 80°C with 1:2(b) and 1:4(d) ratio of CNTs:PEDOT. Composite with 1:4 ratio of CNTs:PEDOT initially dried at room temperature for 36 hours, then heated 80°C for 6 hours(e). The CNTs concentration for all composites is 9.8 wt%.....	30
Figure 3.12 Electrical conductivity of different CNTs concentration with CNTs:Stabilizer 1:4 ratio. The inset is a linear-log plot of the electrical conductivity as a function of the CNTs wt % with two different stabilizers, PEDOT:PSS and GA.	31
Figure 3.13 Thermopower of different CNTs concentration with CNTs:PEDOT:PSS	32
Figure 3.14 Thermal conductivity of different CNTs concentration with CNTs:PEDOT ...	33
Figure 3.15 Electrical conductivity of different ratio and drying condition (CNTs 9.8 wt%).....	34
Figure 3.16 Thermopower of different ratio and drying condition (CNTs 9.8 wt%).....	34
Figure 3.17 Thermal conductivity of different CNTs:PEDOT ratio(CNTs 9.8 wt%).....	36
Figure 3.18 Power factor ($S^2\sigma$) of CNTs concentration (1:4 ratio)...	37

	Page
Figure 3.19 Power factor ($S^2\sigma$) of different ratio and drying condition(CNTs 9.8 wt%).	37
Figure 3.20 ZT of CNTs concentration (1:4 ratio)	38
Figure 3.21 ZT of different CNTs:PEDOT ratio (CNTs 9.8 wt%).	38

NOMENCLATURE

V	Voltage (V)
I	Current (amp)
R	Electrical Resistance (Ω)
S	Seebeck Coefficient or Thermopower (V/K)
D	Thickness of Polymer composite (mm)
A	Cross Section Area of Polymer composite (m^2)
K	Thermal Conductivity (W/m-K)
Σ	Electrical Conductivity (S/m)
P	Electrical resistivity (Ω -m)
ΔV_{TE}	Thermoelectric voltage (V)
ΔT	Temperature difference
Q	Heat flux (W/m^2)
G_{th}	Thermal conductance (W/m^2 -K)
K_f	Thermal conductivity of filler (W/m-K)
K_f	Intrinsic thermal conductivity of filler (W/m-K)

CHAPTER I

INTRODUCTION

The society depends on traditional petroleum-based energy sources. However, people expect that those traditional energy sources will be depleted in near future. For the next two decades, rising global energy demand will lead to a sharp increase, over 50%, in world energy consumption. In July 2008, the world crude oil price was recorded at its highest value. The oil price passed over \$140 per barrel. Since September oil prices decreased under \$100, but they can easily increase again. Nobody can anticipate when another oil crisis will happen to the world¹. Figure 1.1 shows the oil price changes over the last 12 months¹.

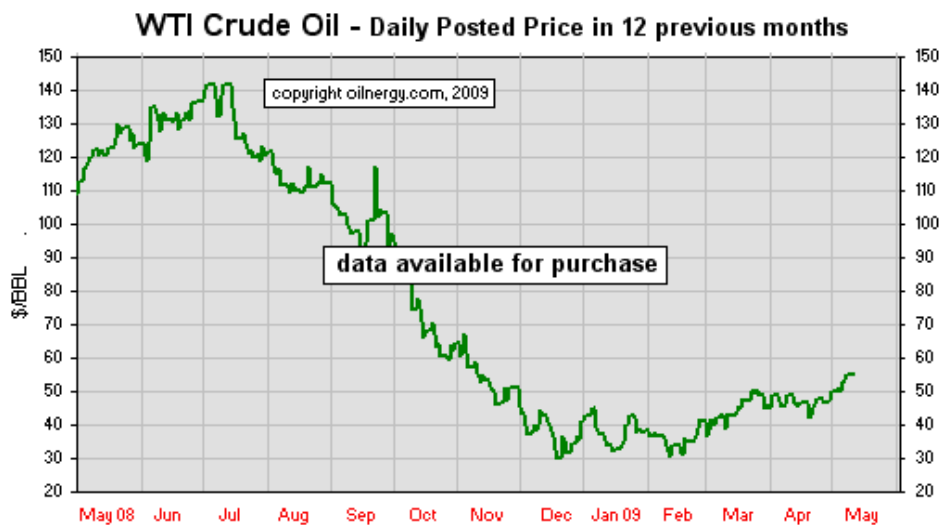


Fig. 1.1 Crude oil price change trends from May 08 ~ May 09

Many countries face severe environmental problems, such as global warming and air pollution due to consuming petroleum-based energy sources. Thus many countries try to find and develop new energy sources which can replace traditional petroleum-based energy sources. They are also interested in new types of energy conversion systems that function without polluting the environment and with low price such as thermoelectric energy conversion.

1.1 Literature Review

Thermoelectric system collects energy by developing a voltage difference when exposed to a temperature gradient^{2, 3}. Thermoelectrics have several advantages over conventional methods used to generate electricity. It is environmentally safe and mechanically robust because there are no moving parts⁴.

In most system there are some kinds of waste heat. This heat can be converted into useful electrical energy using thermoelectric system. Figure 1.2 shows a diagram of thermoelectric energy conversion with waste heat. One example of a possible thermoelectric application can be found in the automobile industry. Passenger vehicles lose over 60% of total fuel as waste heat through the engine radiation and the exhaust system⁵. Once a thermoelectric generator is formulated, this waste heat can be directly converted to electricity in the inner vehicle system, which can be used to operate the electrical system or recharge a hybrid vehicle's engine battery resulting in reduced fuel consumption. The main obstacle for thermoelectric systems is the low efficiency of thermoelectric material. The efficiency of thermoelectric materials is expressed by the thermoelectric figure of merit, ZT

that is defined as

$$ZT = \frac{S^2 \sigma T}{k}$$

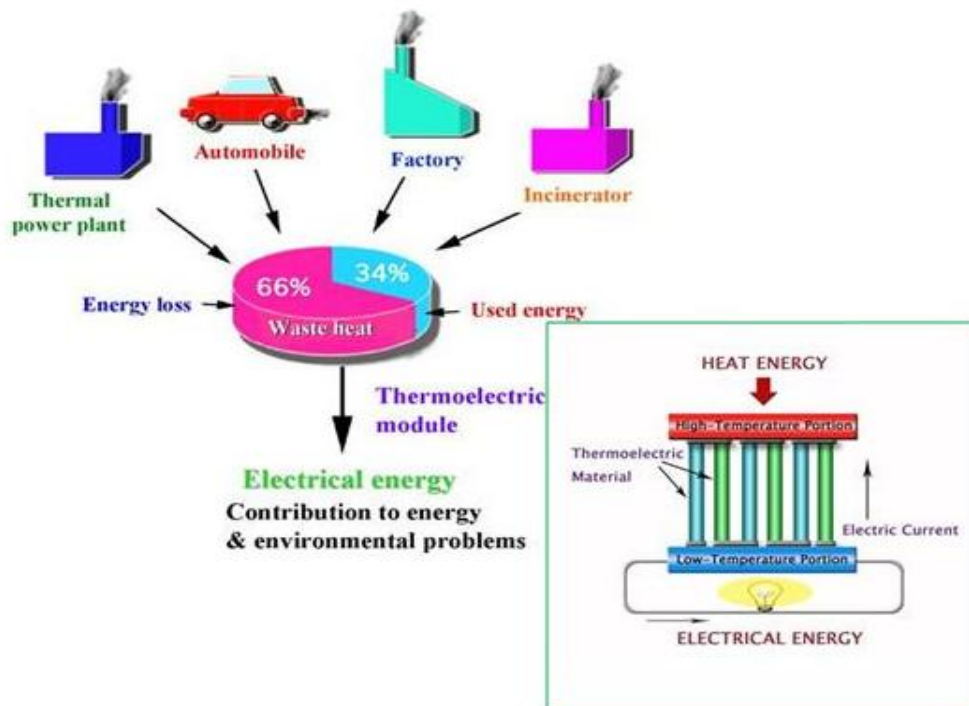


Fig. 1.2 Diagram of thermoelectric energy conversion with waste heat

where S is the Seebeck coefficient (thermopower), σ is the electrical conductivity, k is the thermal conductivity and T is the absolute temperature. In order to achieve a high ZT , it is necessary to obtain a large S and σ , but small k . These three properties, however, are strongly correlated in bulk crystalline materials. Changing one parameter favorably often makes the others undesirable.

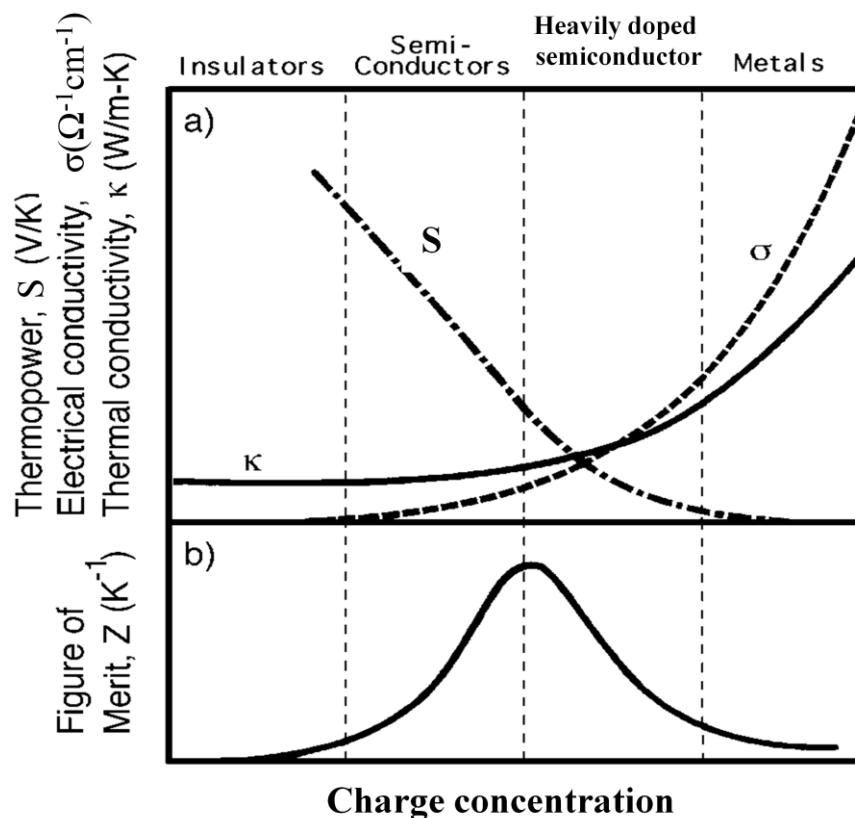


Fig. 1.3 Relationship between thermoelectric properties and their dependence on carrier concentration

Figure 1.3 shows the relationship between thermoelectric properties and charge carrier concentration in bulk crystalline materials. As more charge carriers are added, electrical conductivity increases linearly while the Seebeck coefficient decreases. ZT reaches a maximum in the middle of the carrier concentration⁶. The thermal conductivity can be broken into two parts, electrical and phonon: Phonons are quantized vibration modes of energy due to crystal vibrations. This term does not depend on charge carriers and remains constant. In many semiconductor materials the phonon contribution to the thermal

conductivity is significantly higher than electrical contribution even at large carrier concentrations⁷. One possible way of maximizing ZT is to decrease thermal conductivity. This can be done effectively by suppressing k_{phonon} without significantly disturbing k_{electron} . In general, polymers are not a suitable materials for thermoelectrics because they have a low electrical conductivity. However, by embedding electrically conductive filler, polymer composites can significantly increase electrical conductivity without sacrificing their thermal conductivity and thermopower⁸⁻¹⁰. Figure 1.4 shows the trends of these thermoelectric properties of segregated network polymer composites. The electrical conductivity significantly increased, but thermal conductivity and thermopower doesn't change a lot. These behaviors comes from thermally disconnected, electrically connected many junctions of nanotubes. This segregated network polymer composites consist of carbon nanotubes (CNTs) and poly (vinyl acetate) (PAVc) exhibits a thermoelectric figure of merit (ZT) of 0.01 at room temperature showing that the conductive polymer composites can be viable as a lightweight and economical thermoelectric material¹¹.

Carbon nanotubes tend to aggregate into tangled networks due to strong Van de Waals attraction between nanotubes^{12, 13}. Highly entangled carbon nanotubes are difficult to disperse in water and could be harmful for inter-tube charge transport¹⁴. It has been demonstrated that the tunneling of electrons between nearest-neighbor nanotubes dictates the onset of electrical percolation and thus the value of the inter-tube distance is of great importance¹⁵.

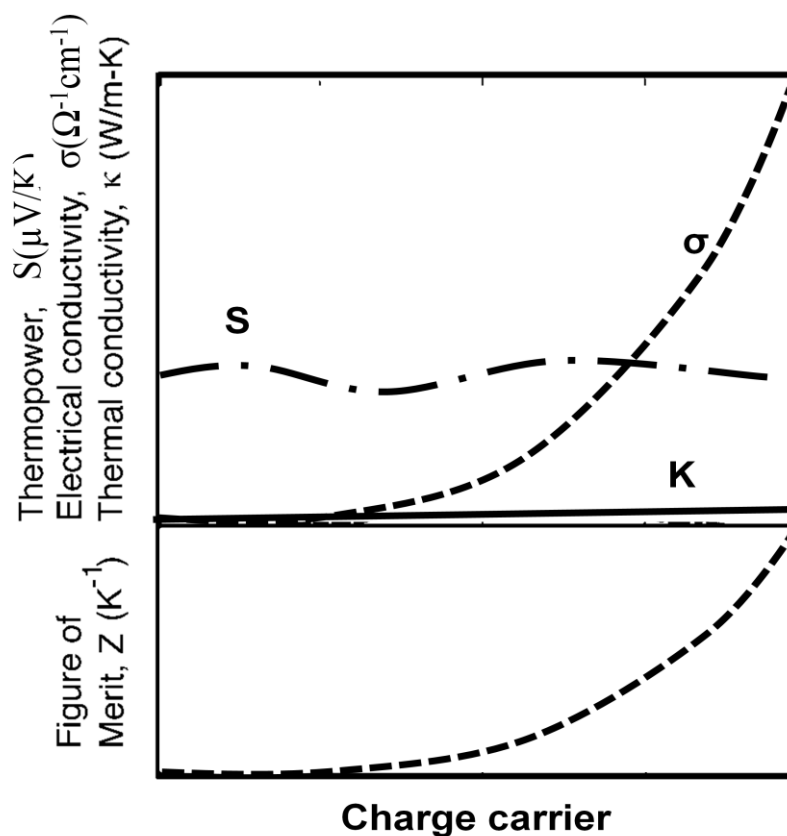


Fig. 1.4 Relationship between thermoelectric properties of segregated network polymer composites and their dependence on carrier concentration

Electron tunneling distance is influenced by the electronic states of the CNTs, the contact potential barrier and the electrostatic charging of the CNTs and the polymer matrix¹⁶. There are several types of stabilizing agents that have been adapted such as surfactant, polymer, and inorganic clay¹⁷. These agents, however, are electrical insulators that hinder the electrical transport behavior of composites. If a conductive polymer is used to replace these conventional stabilizing agents, the transport properties of composite would be significantly enhanced. In this work, poly (3, 4-ethylene dioxythiophene): poly (styrene

sulfonate) (PEDOT:PSS) doped with dimethyl sulfoxide (DMSO) is used to disperse CNTs in water. PEDOT:PSS¹⁸⁻²¹ has been widely used as an antistatic coating material, as electrodes for capacitors or photodiodes, and as a hole transport layer in organic LEDs^{22,23}. Its electrical conductivity is typically between 10^5 and 10^6 S/m at room temperature^{24, 25}. Adding this electrically conductive polymer when introduced into the latex based matrix for segregated network composites could significantly reduce the non-contact resistivity between adjacent CNTs. The high affinity of conjugated polymers for CNTs through π - π electronic interactions ensures a close conductive polymer-CNTs contact²⁶. PEDOT:PSS, which can act as a polymeric surfactant has been reported to effectively disperse CNTs in water²⁷.

1.2 Research Objective

In this thesis, we introduce segregated network of CNTs that were implemented by using emulsion polymers as a matrix to maximize the network electrical conductivity. This method uses aqueous polymer emulsions, whose particles create excluded volume and essentially push carbon nanotubes into the interstitial space between them. This situation dramatically reduces the space available for the carbon nanotubes to form conductive networks, which results in a significant enhancement of electrical conduction with a relatively small amount of electrically conductive filler.²⁸ The electrical conductivity of polymer composites can be as high as the electrical conductivity of typical semiconductors, but have significantly lower thermal conductivity which is close to the intrinsic polymer's value. Moreover, the Seebeck coefficient of the conductive polymer composites is

independent of filler concentration so it can achieve high electrical conductivity without sacrificing Seebeck coefficient.

The main purpose of this thesis is three fold : (1) to demonstrate that segregated network polymer-CNT nanocomposites can be viable as a light weight and economical thermoelectric material (2) to investigate the transport behavior of CNT-filled nanocomposites with different amount of stabilizing agent (3) and to enhance the thermoelectric properties of polymer-CNTs nanocomposites by changing the stabilizer and drying conditions.

CHAPTER II

EXPERIMENTAL PROCEDURE

Polymer particles create excluded volume and push electrical fillers into the interstitial space between polymer particles. Fig. 2.1 shows a schematic of CNTs and polymer particles suspended in an aqueous emulsion.

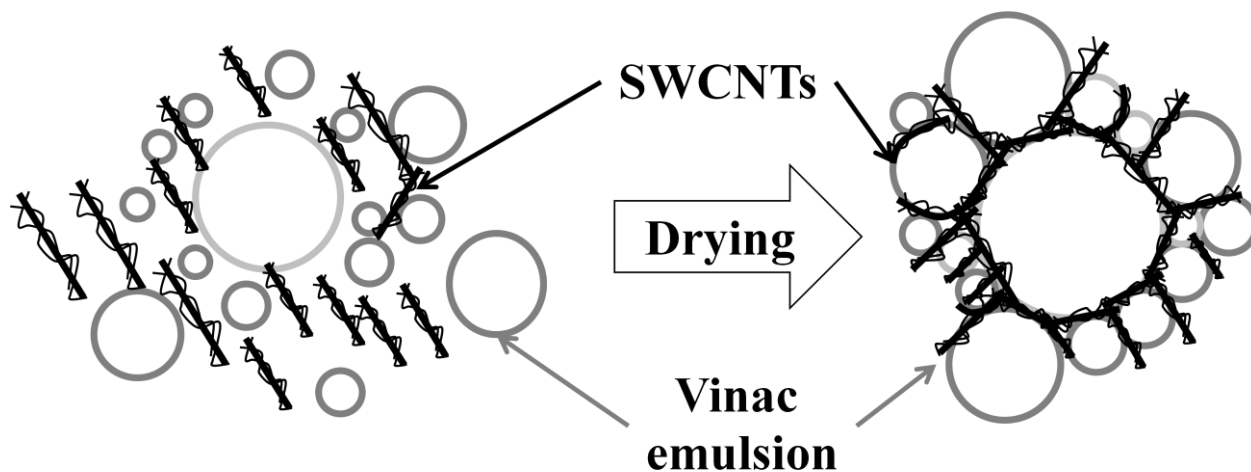


Fig. 2.1 Microstructure of segregated network polymer-CNTs nanocomposite

Gray spheres and black lines represent emulsion particles and CNTs, respectively. The right side of the schematic shows the emulsion-based composite after drying. The CNTs form a three-dimensional network along the surfaces of the spherical emulsion particles.

2.1 Composite Materials

2.1.1 CNTs Filled with Vinac Emulsion (Stabilizer: Gum Arabic)

The composite matrix was made from a poly (vinyl acetate) (PVAc) homopolymer emulsion (Vinac XX210 Emulsion) (Air Products, Inc.) that was 55.16 wt % solids in water. A polymer emulsion is made up of spherical polymer particles in water prior to film formation. The particle size distribution is 0.14-3.5 μm with an average diameter of ~ 650 nm. The glass transition temperature (T_g) of vinac emulsion is 35° C, so it has glassy behavior at room temperature. Purified SWCNTs which were produced by the HiPco process and contain 5wt % of impurities (purchased from Carbon Nanotechnologies Inc., Houston, TX) were incorporated in the polymer matrix. Gum Arabic (GA) (Sigma-Aldrich, Co.) was used to disperse the CNT in water. For this study, seven different CNT concentrations, 1, 2, 3, 4, 5, 10 and 20 wt%, in vinac emulsion were prepared. These concentrations are based on the total dry weight of the composite, which includes CNTs, vinac emulsion and GA. Four different ratios between CNTs and GA, 10:1, 3:1, 1:1 and 1:3 at CNTs 3 and 10 wt % were also prepared to see the influence of stabilizer.

2.1.2 CNTs Filled with Airflex Emulsion (Stabilizer: PEDOT:PSS)

In this experiment, different stabilizers were used to enhance thermoelectric properties. By replacing electrically non-conductive GA with highly conductive PEDOT:PSS, whose electrical conductivity ranges typically 10^5 S/m at room temperature.^{24, 29, 30}. The composite matrix was made from Airflex @ 401 Emulsion (Air Products, Inc.) which is a mixture of poly (vinyl acetate) (PVAc) and poly ethylene (PE) copolymer

emulsion that was 55.16 wt % solids in water. A polymer emulsion is a stable suspension of spherical solid, polymer particles in water prior to film formation. The low glass transition temperature (T_g) of airflex was -15°C , so it's more flexible than Vinac XX210 (T_g 35°C) that was used for the composite reported earlier. XM grade CNTs (Carbon Nanotechnologies, Inc.), which are a mixture of metallic and semiconducting single-, double-, and triple-walled CNTs, were incorporated into the matrix. Gum Arabic (GA) (Sigma-Aldrich, Co.) or PEDOT:PSS (Poly (3, 4-ethylenedioxythiophene) poly (styrenesulfonate)) that was 1.3 wt % solids in water were used to stabilize the CNT in water.³¹ PEDOT:PSS dispersions (CLEVIOS™ P, H. C. Starck) contain 0.5 wt% PEDOT and 0.8 wt% PSS. In order to increase electrical conductivity, PEDOT:PSS was doped with Dimethyl sulfoxide (DMSO, Sigma-Aldrich, Co.) for 2 hours before sample synthesis.³² For this study, six different CNT concentrations, 2.1, 4.4, 6.9, 9.8, 12.5 and 15 wt% with 1:4 ratio of CNTs and PEDOT:PSS in airflex emulsion were prepared to study the influence of CNTs. And four different ratios between CNTs and PEDOT:PSS, 1:1, 1:2, 1:3 and 1:4 were prepared. At last, three different drying conditions, room temperature, 80°C and combination of room temperature and 80°C were prepared to compare the change in electrical conductivity.³³ One condition is room temperature for 5 days and another is 80°C for 6 hours.

2.2 Composite Formation

In order to prepare the polymer-CNTs composites, dry CNTs were mixed with 2 wt% solutions of GA by sonication with a VirTis Virsonic 100 ultrasonic cell disrupter (SP

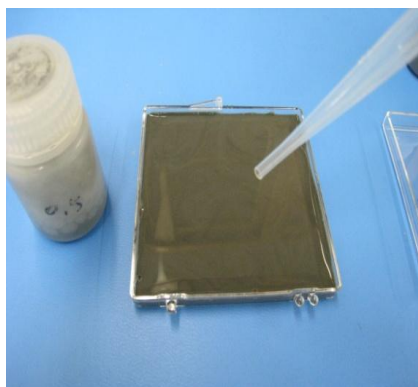
industries, Inc.) for 15 min at 50 W. The CNT and GA weight ratio was 1:1. The vinac emulsion and de-ionized water were added to the CNT/GA mixture to produce a composite mixture, after a 5-min sonication. For this study, seven different CNT concentrations, 1, 2, 3, 4, 5, 10, and 20 wt% in vinac emulsion were prepared. In addition, 0 wt% CNT polymer sample was also synthesized to compare its thermoelectric properties. Composites were made by drying mixtures in a 29 cm² square plastic mold for two days under ambient conditions and then for 24 hours in a vacuum desiccator to completely remove air and moisture. Figure 2.2 shows the way how to synthesize the composites.



a) Mix the ingredients of sample



b) Sonication for sample



c) Pour sample to mold (2x2 inch)



d) Dry sample under Desiccator

Fig. 2.2 Synthesis of composites in emulsion matrix

In the second experiment, to prepare the composites, PEDOT:PSS solution and DMSO were mixed for doping and shaken for 2 hours. Dry CNTs were combined with doped PEDOT:PSS solutions by sonication with a VirTis Virsonic 100 ultrasonic cell disrupter (SP industries, Inc.) for 15 min at 50 W. The CNT had a 1:4 weight ratio with PEDOT:PSS. The airflex emulsion and de-ionized water were then added to the PEDOT:PSS/CNT mixture to produce an aqueous pre-composite mixture, followed by 5-min sonication. For this study, six different CNT concentrations, 2.1, 4.4, 6.9, 9.8, 12.5, and 15 wt% in airflex were prepared. Solid composites were made by drying aqueous mixtures in a 29 cm² square plastic mold for five days under ambient conditions and then for 24 hours in a vacuum desiccators. In addition, different drying conditions were tried to compare the change in thermoelectric properties. After sonication, the mixture was dried for 36 hours under ambient condition and for 6 hours in elevated temperature(80°C) and then for 24 hours in a vacuum desiccator.

2.3 Composite Characterization

For electrical conductivity and thermopower measurements, samples were cut into pieces (typically ~30 mm × ~6 mm). Another set of circular samples with 25.4 mm in diameter were prepared for thermal conductivity measurements. Figure 2.3 shows an example of sample preparation for thermoelectric properties measurement. Figure 2.4 shows the experimental equipment for thermoelectric properties measurement.

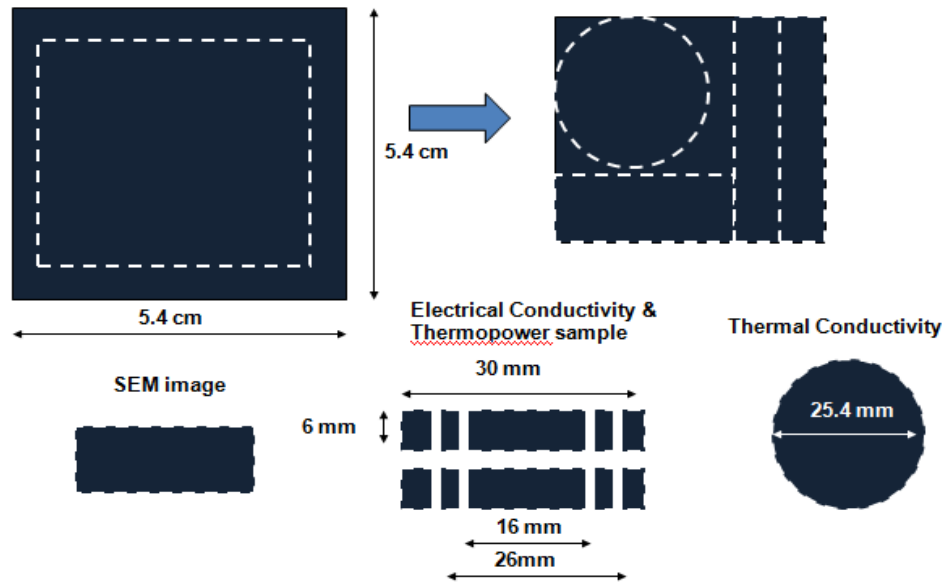


Fig. 2.3 Sample preparation for thermoelectric properties measurement

2.3.1 Electrical Conductivity and Thermopower

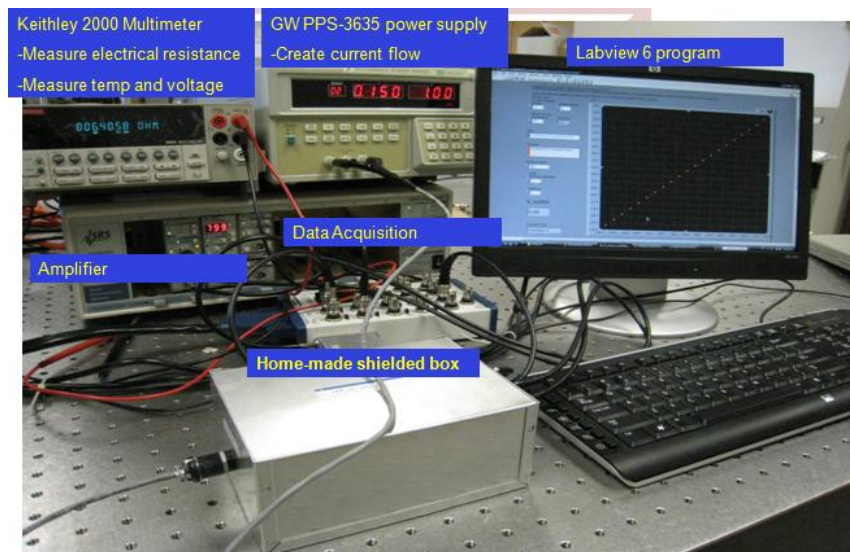


Fig. 2.4 Experimental equipment for thermoelectric properties measurement

At both ends of the samples, four conductive metal lines were attached to the sample for current-voltage (I-V) measurements. Electrical resistance was obtained by taking the slope of the I-V curve and converting it into electrical conductivity by calculating a geometric factor (length, width and height).

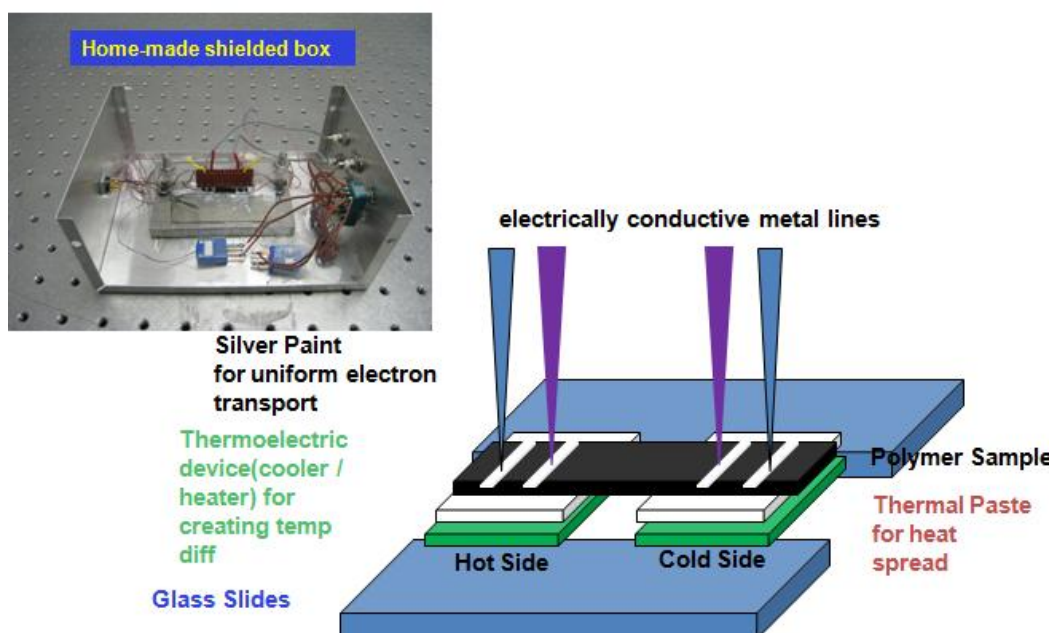


Fig. 2.5 Home-made shielded box and scheme for thermopower measurement

Next, to create temperature gradients the samples were suspended on two thermoelectric devices. When the temperature gradient was varied, thermoelectric voltages were measured and thermopower (S) was obtained from the slope ($S = \Delta V_{TE} / \Delta T$, where ΔV_{TE} and ΔT are the thermoelectric voltage and temperature). The electrical conductivity and thermopower measurements were done with the same sample. Because these two

parameters are strongly correlated, this minimizes the error that might be present due to the difference of microstructures and CNT concentrations over the whole sample. Figure 2.5 shows experimental equipment for electrical conductivity and thermopower measurement.

2.3.2 Thermal Conductivity

The sample with 25.4 mm in diameter was clamped between two stainless steel rods whose ends were heated to 50°C and cooled to 0°C, for creating temperature gradients along the out of plane direction of the sample. Five thermocouples were embedded along the vertical direction of each rod and used to determine q and ΔT in the thermal conductance relation ($G_{th} = q/\Delta T$, where G_{th} and q are thermal conductance per unit area (W/K-m²) and heat flux (W/m²). The temperature difference (ΔT) between two rods was obtained by the series of temperature measurements and was typically ~4 K. The thermal conductivity of the sample was obtained from $k = t \times G_{th}$, where t is the thickness of the sample. In order to prevent heat losses to the environment, such as convection and radiation, the stainless steel rods were covered with polymeric thermal insulator. Figure 2.6 and 2.7 show experimental setup for thermal conductivity measurement.

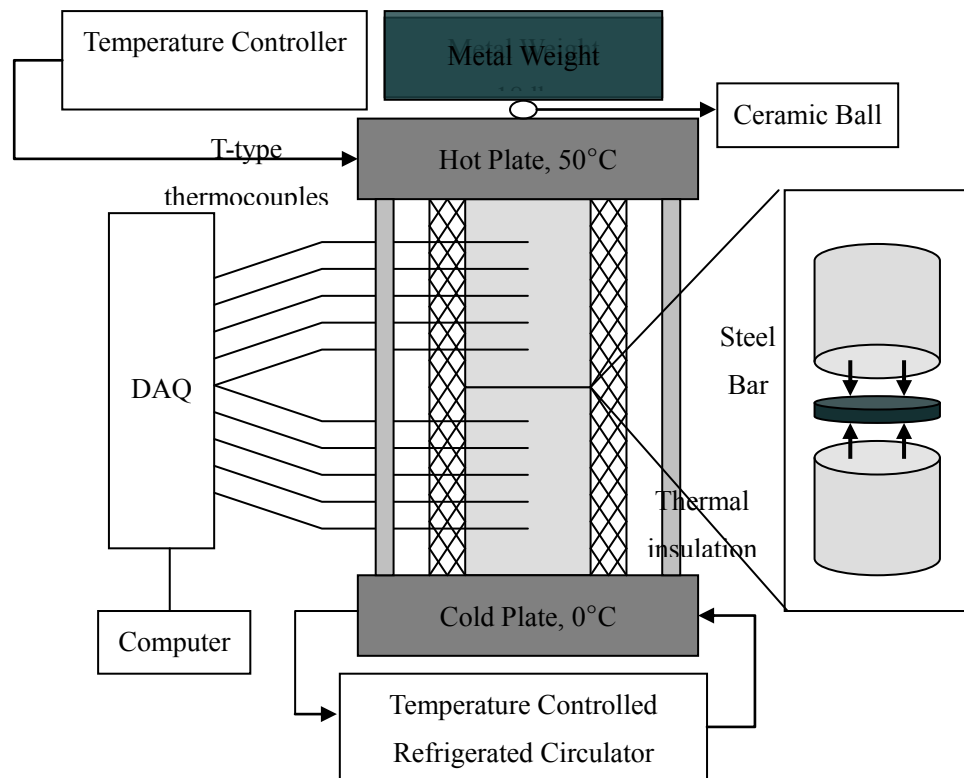


Fig. 2.6 Schematic diagram of the setup to measure thermal conductivity

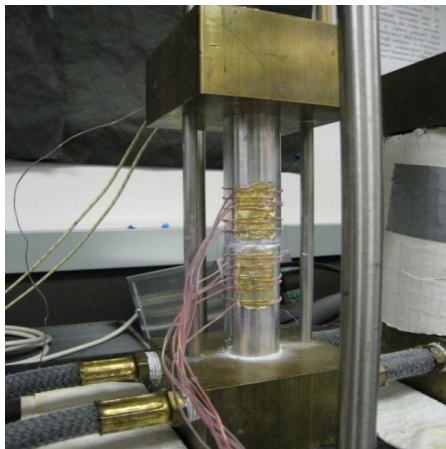


Fig. 2.7 Experimental setup. Stainless steel rod and thermocouples

CHAPTER III

RESULTS AND DISCUSSION

3.1 CNTs Filled with Vinac Emulsion (Stabilizer: GA)

The benefit of segregated network composites comes from the existence of CNT junctions that significantly impede thermal transport. The network structure allows most of the CNTs to contribute to the electrical conduction as opposed to homogeneous nanocomposites, so as to maximize the influence from the filler..

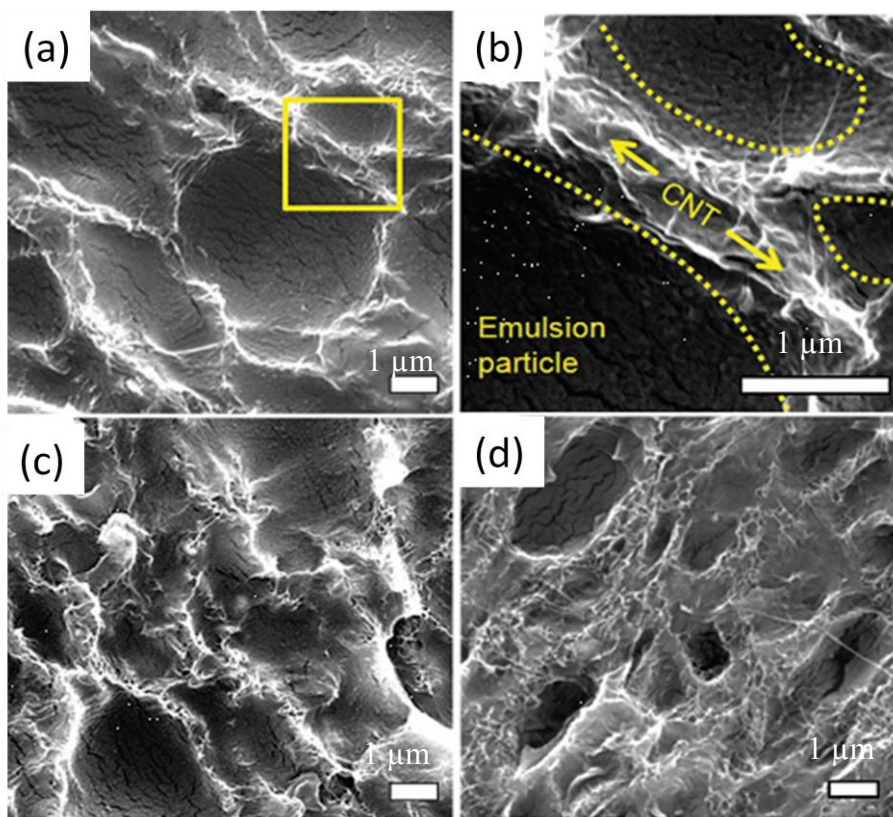


Fig. 3.1 SEM images of 5 (a), 5 (b), 10(c) and 20(d) wt% of CNTs

In figure 3.1 (a) and (b), SEM images shown in panel (b) are a portion of the sample in (a) indicated by a solid yellow square. It clearly shows that CNTs (indicated by arrows) are wrapped around the emulsion particles (indicated by yellow dotted lines) rather than homogeneously mixed. Denser CNTs were observed for higher concentration CNT composites.

Figure 3.2 shows the electrical conductivity and thermopower of 1, 2, 3, 4, 5, 10, and 20 wt% composites at room temperature. When CNTs were added to the composite above 4 wt%, the electrical conductivity was dramatically increased. At 20 wt%, electrical conductivity was ~ 4938.8 S/m, which is much higher than the typical 1~10 S/m values obtained in previous nanotube-filled polymer composites with a similar concentration³⁴. Despite this large increase in electrical conductivity, thermopower kept relatively constant (40~50 μ V/K). This value is close to the thermopower of a metallic CNT, as thermopower does not depend on filler dimensions and is strongly affected by more electrically conductive paths. This feature is ideal for tailoring thermoelectric properties because the electrical conductivity can be increased without sacrificing thermopower and thermal conductivity, which is the opposite of the behavior observed in bulk crystalline materials. From the values of the thermoelectric parameters shown in Figure 3.2 and 3.3, ZT of the composite was calculated to be ~ 0.006 at 300 K, which is at least 6 times greater than attempts with other polymers. Figure 3.4 shows the thermal conductivity of the composite. In general, CNTs have a thermal conductivity of about 200 W/m-K and the polymer has 0.2 W/m-k. This large gap in k likely comes from the many connections between CNTs along the long chain. They are often connected in series by weak van der Waals forces, which are

expected to play an important role in impeding phonon transport at the connected junctions. This may also be a rationale of many thermal conductivity measurement results of CNT bundles that were lower values than those theoretically predicted.³⁵⁻⁴⁰ Therefore, k'_f is smaller than the intrinsic property (k_f) of the filler material (i.e., $k'_f < k_f$ in the segregated network composite).^{41, 42} This implies that the concentration of the electrically conductive filler can be increased without raising the composite thermal conductivity, which is favorable for the enhancement of the thermoelectric performance that is indicated by the thermoelectric figure of merit.

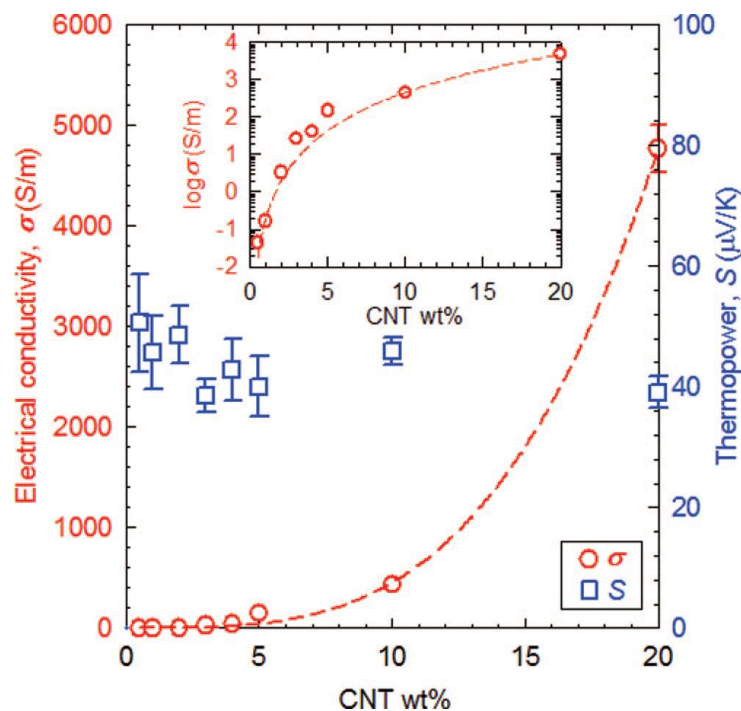


Fig. 3.2 Electrical conductivities and thermopower of CNTs filled with vinac emulsion (Stabilizer: GA). The inset is a linear-log plot of the electrical conductivity as a function of the CNT wt %

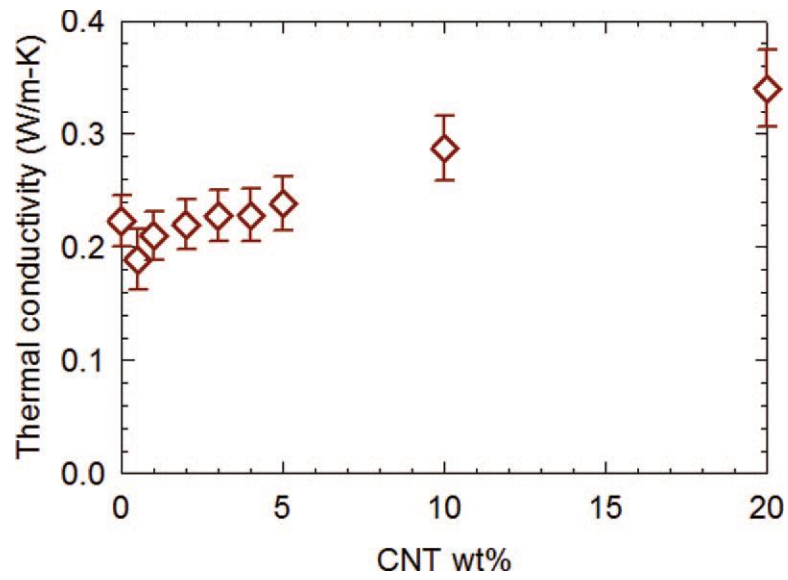


Fig. 3.3 Thermal conductivities CNTs filled with vinac emulsion (Stabilizer: GA)

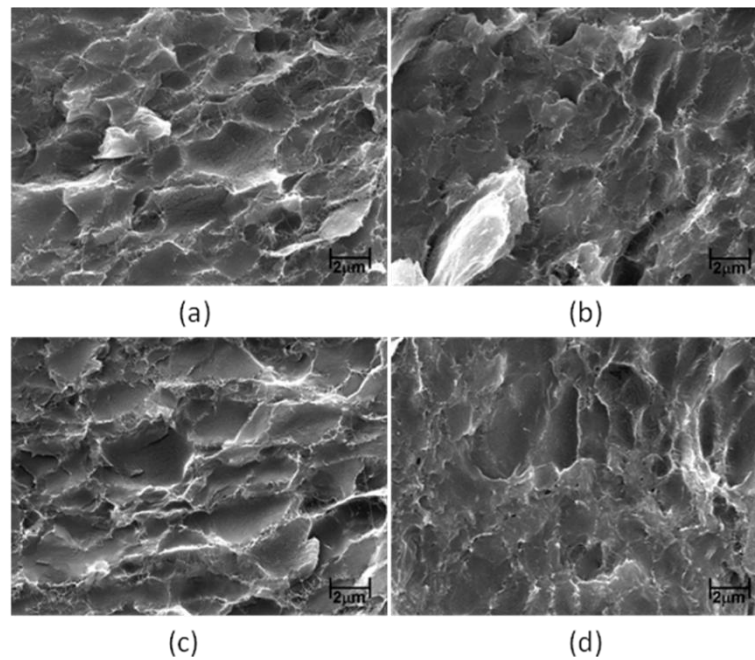


Fig. 3.4 SEM images of 10 wt% of CNTs with 10:1 (a), 3:1 (b), 1:1(c) and 1:3(d) CNTs:GA ratio

The differences in composite microstructure with various amounts of GA are shown in Fig. 3.4. When the GA concentration is minimum (Fig.3.4 (a)), the interaction between CNTs and the polymer matrix is much weaker than in the other composites. Many CNTs are pulled out of the matrix during the freeze-fracture sample preparation process. As the amount GA increases, the CNTs are bonded to the matrix strongly. In the case of 1:3 CNTs:GA ratio in Figure 3.4 (d), CNTs are much more embedded in the polymer matrix with very little pull-out. The dispersion level of CNTs in the matrix is, however, very similar to each other regardless of the GA amount. The concentration of CNTs is the same for all composites. As a result, GA and CNTs are restricted to the interstitial space between polymer particles without hindering the formation of the segregated network microstructure.

The electrical and thermal conductivities of the composites were measured to investigate the influence of the GA on transport behavior. Figure 3.5 shows the electrical conductivity of the composites containing 3 and 10 wt% CNTs with varying CNTs:GA ratio. The electrical conductivity decreases as the amount of GA increases in both 3 and 10 wt% composites. In general, the electrical conductivity is strongly affected by filler dispersion, junctions between fillers and interactions between fillers and matrix. The filler dispersion level determines the number of connecting point between filler particles. The number of junctions and interactions could considerably interfere with the electrical conduction. The GA stabilizer and matrix are electrical insulators and consequently electrical conduction only occurs through CNTs that may interact with the polymer matrix. This interference is reflected in the increase in the film electrical conductivity as the CNT ratio becomes higher.

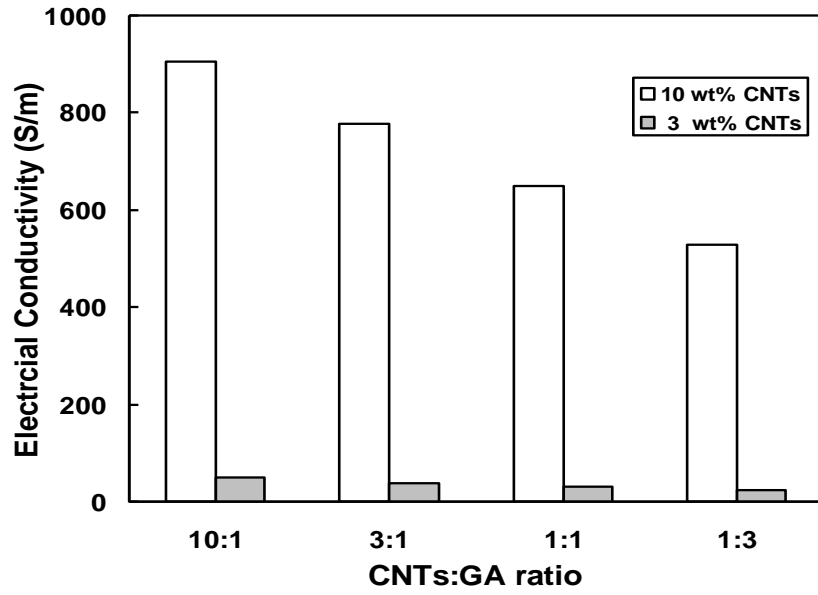


Fig. 3.5 Electrical conductivity of 10 and 3 wt% nanotube-filled composites with different CNTs:GA ratio

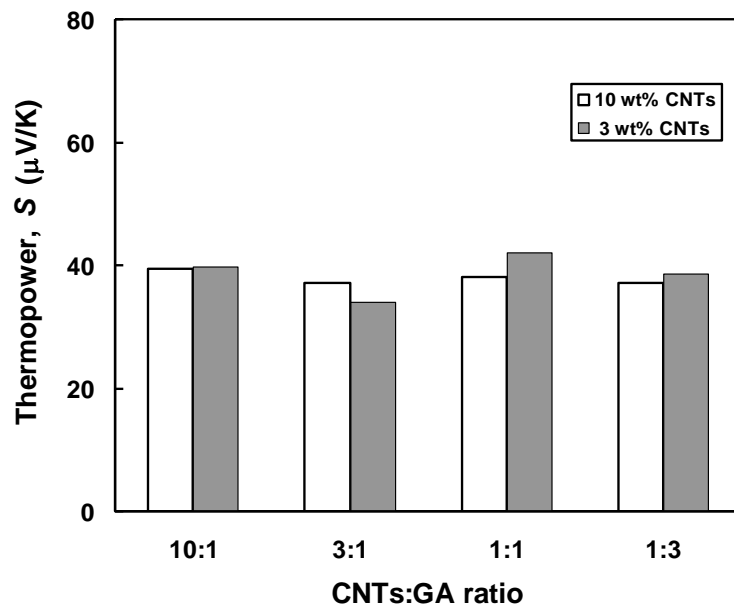


Fig. 3.6 Thermopower of 10 and 3 wt% nanotube-filled composites with different CNTs:GA ratio

The GA is consumed in wrapping CNTs, resulting in a thicker layer of GA around the CNTs for the high GA concentration samples. The insulating GA essentially acts as a barrier for electron transport, decreasing the number of electrons that are transported across the tube-junctions. The phenomena were well expressed in the increase of electrical conductivity with less GA concentration. On the other hand, Fig. 3.6 shows that the thermopower of all samples are similar.

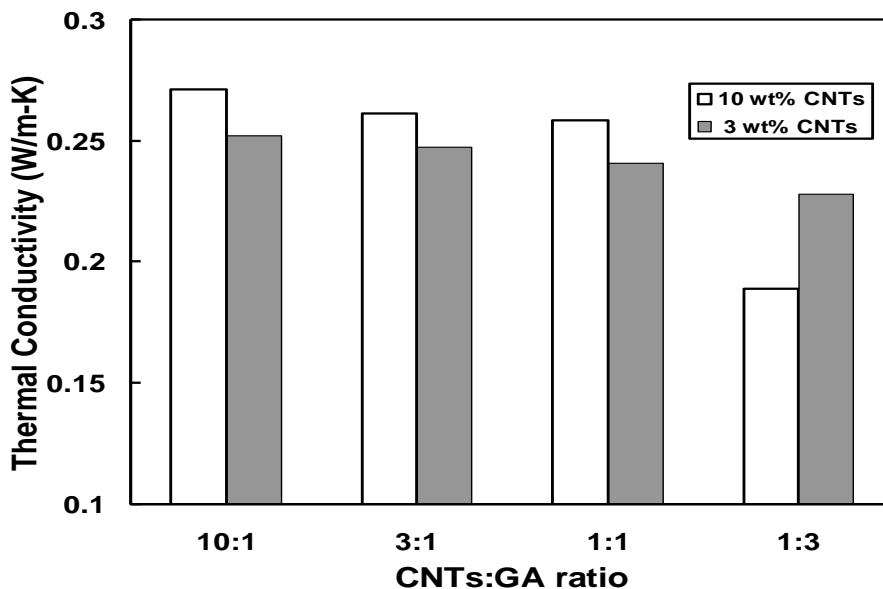


Fig. 3.7 Thermal conductivity of 10 and 3 wt% nanotube-filled composites with different CNTs:GA ratio

Thermal conductivities of 3 and 10 wt% CNTs composites decrease with increase in GA concentrations as shown in Figure 3.7 due to the thicker GA coating layer on the CNTs surface. The GA between CNTs creates diffusive soft junctions, resulting in low thermal

conductivity due to acoustic impedance mismatches. Furthermore, the CNTs and coating layer are bonded by a weak van der Waals force. While the indirect contact of fillers and weak bonding effectively impede the phonon transport, the electrical conductivity can be maintained by other type of transport mechanism such as electron hopping and tunneling without direct contact between nanotube bundles. Fig. 3.8 shows the calculated ZT, thermoelectric figure of merits, at room temperature.

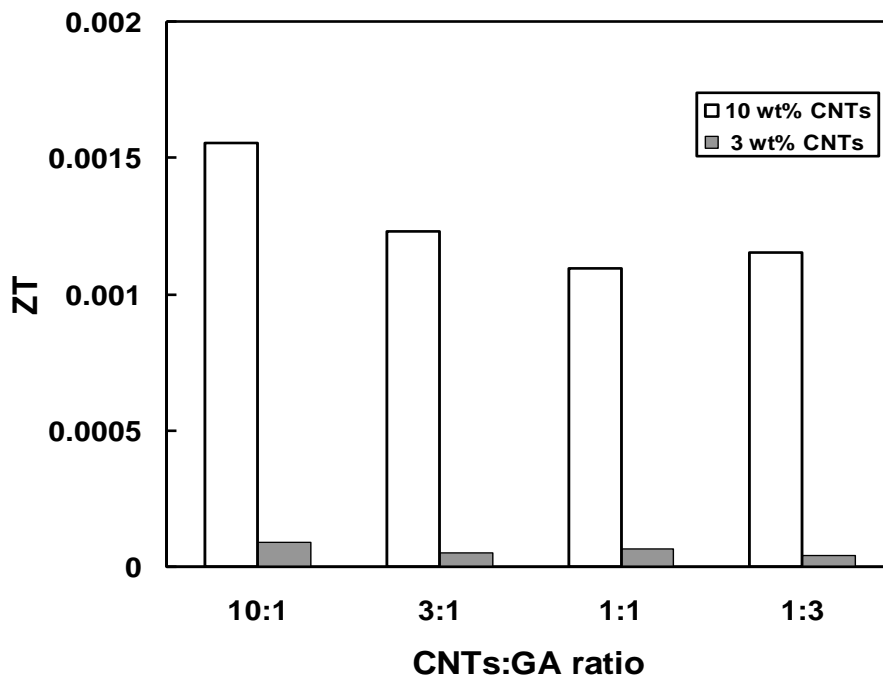


Fig. 3.8 Calculated ZT of 10 and 3 wt% nanotube-filled composites with different CNTs:GA ratio

3.2 CNTs Filled with Airflex Emulsion (Stabilizer: PEDOT:PSS)

The introduction of PEDOT:PSS leads to the bridging of some tube junctions and the composite conductivity increases. As a result, an increasing loading of PEDOT:PSS increases the number of bridged junctions until a point at which the conductivity becomes similar to that for the completely covered tubes. The PEDOT:PSS forms junctions between adjacent tubes at sufficiently high loadings.

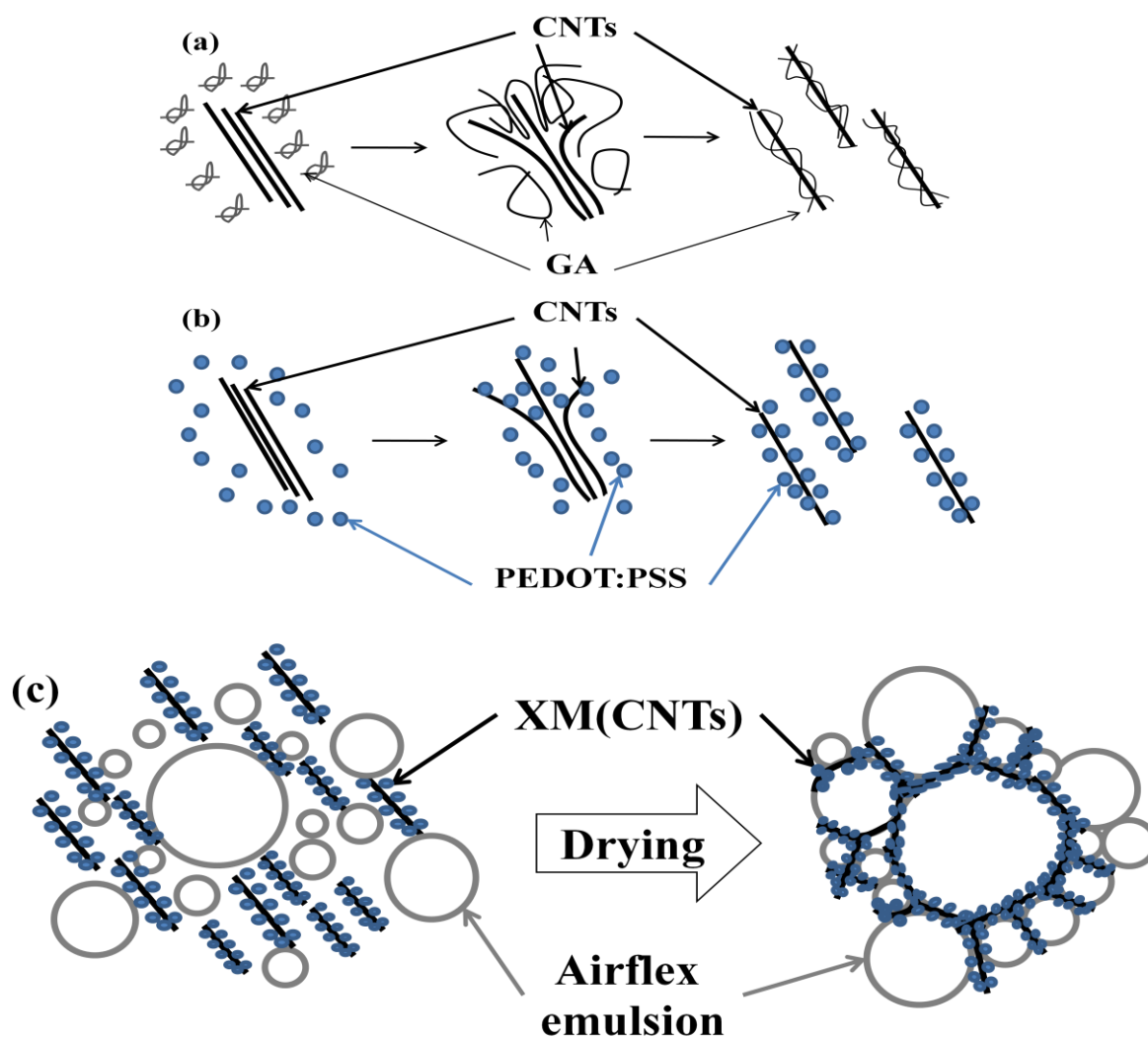


Fig. 3.9 Schematic of function of Gum Arabic (a) and PEDOT:PSS (b) and dispersed by PEDOT:PSS in aqueous emulsion as stabilizer (c)

Figure 3.9 shows a schematic of Gum Arabic (a), PEDOT:PSS (b) and the drying of CNTs dispersed by PEDOT:PSS in an airflex emulsion as stabilizer (c). Composite samples were freeze-fractured for microstructure analysis. Figure 3.10 shows the SEM images of composites cross-section containing CNTs stabilized by PEDOT:PSS. PEDOT:PSS particles are shown as bright dots in the SEM images. Well developed networks of CNTs along with PEDOT:PSS particles are observed for all concentrations. It is clearly seen that PEDOT:PSS used to stabilize the CNTs in water effectively exfoliates the CNTs. At the concentration of 4.4 wt%, most CNTs are embedded within the polymer matrix showing that the interaction between CNTs and the polymer matrix is strong. As the concentration increases up to 15 wt%, the network becomes thicker and many CNTs are pulled out from the matrix. Increasing composite porosity is also observed with higher CNT concentration. Micro voids start to form when the polymer emulsion particles cannot envelop the filler due to high filler concentration. These microstructure images, however, show that this system is able to incorporate more filler than the previous series where Single-Walled Carbon nanotubes and vinac emulsion were used as filler and matrix. The CNTs used in this study were an XM grade, which is a mixture of single-, double-, and tri-walled CNTs. XM grade CNTs have less surface area than SWNT so that larger amounts of CNTs can be mixed with the polymer matrix. More importantly, the airflex has a lower glass transition temperature indicating that the matrix is much softer than the vinac at drying temperature. It is known that the softer polymer emulsion has the ability to contain more filler than the hard emulsion when they are dried at the same temperature.

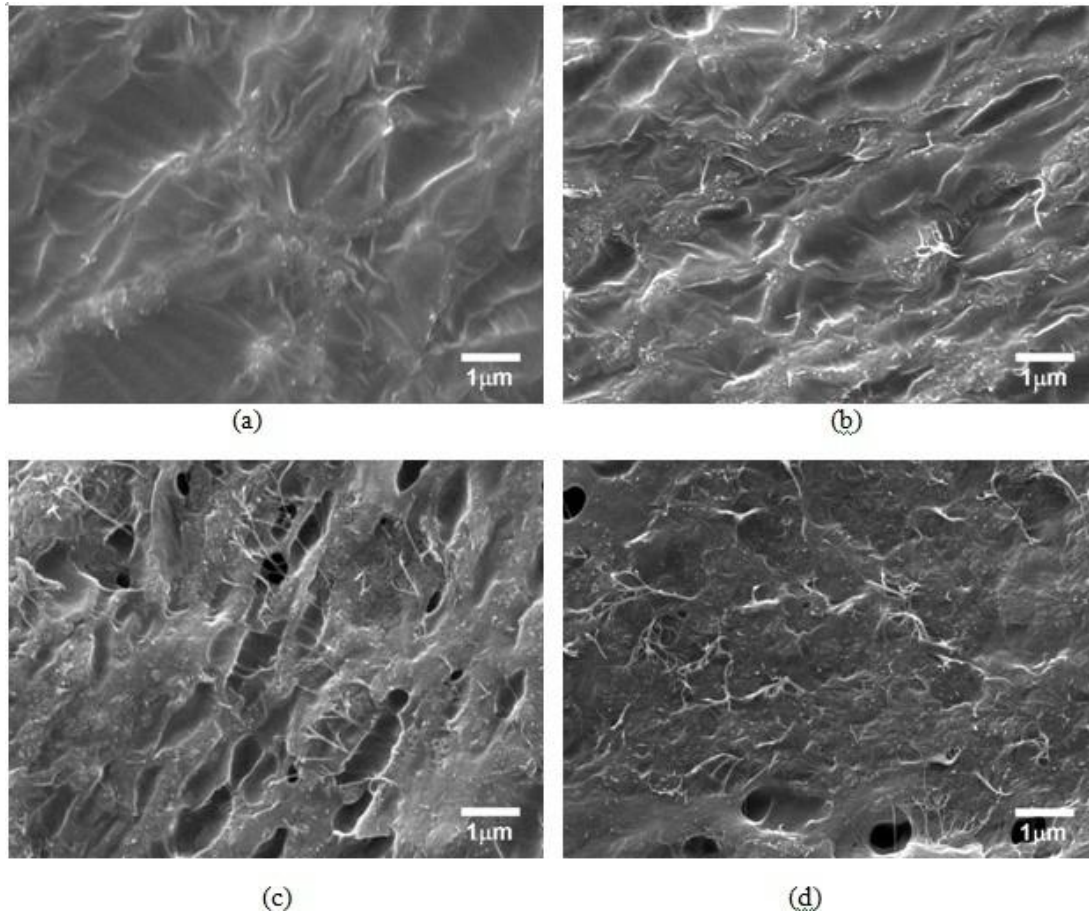


Fig. 3.10 SEM cross-section of a 4.4 wt% CNT composite after the composite was freeze-fractured. SEM images of the cross-sections of 6.9, 12.5 and 15 wt% CNT composites are shown in (b), (c) and (d). The ratio between CNT and PEDOT is 1 to 4.

It is important to find the optimal ratio of CNTs to PEDOT:PSS to achieve the best property enhancement. Microstructures of composites containing 9.8 wt% CNT with ratios of 1:2 and 1:4 of CNT to PEDOT:PSS are given in Figure 3.11 (a) and (c). It is not obvious how the amount of PEDOT:PSS affect the CNT dispersion with these micrographs because the SEM images only show the surface of the samples, but the 1:4 composite clearly shows the heavier aggregation of PEDOT:PSS particles with a higher level of porosity. Even

though PEDOT:PSS is a polymeric material, it is a solid particle increasing the overall filler concentration that causes void formation. Composites are also dried at elevated temperature (80°C) to examine the effect of drying on film properties. Composites dried at 80°C show much smoother surfaces and stronger interactions between CNTs and the matrix, especially in the 1:4 composite. Most of CNTs are embedded in the polymer matrix and the voids are nearly eliminated when the composites are dried at 80°C. This is due to the lower modulus of the emulsion polymer at higher temperature. When the modulus of the polymer decreases, the emulsion particles are able to more effectively deform and fill the gap between the CNTs. Combination of room temperature and 80°C drying conditions was also attempted. The composite was allowed to dry at ambient temperature for 36 hours initially, and then heated to 80°C for an additional six hours. As shown in the figure (e), the microstructure of the composite dried at combination condition is very similar with that of elevated temperature dried composites.

Figure 3.12 shows the electrical conductivity of 2.1, 4.4, 6.9, 9.8, 12.5 and 15 wt % CNT composites with 1:4 ratio for CNTs and PEDOT:PSS at room temperature. The linear-log scale inset indicates that the composites with PEDOT:PSS as stabilizer resulted in an increase of electrical conductivity by as much as several thousand times the one with GA in ratio of 1:4 for both.

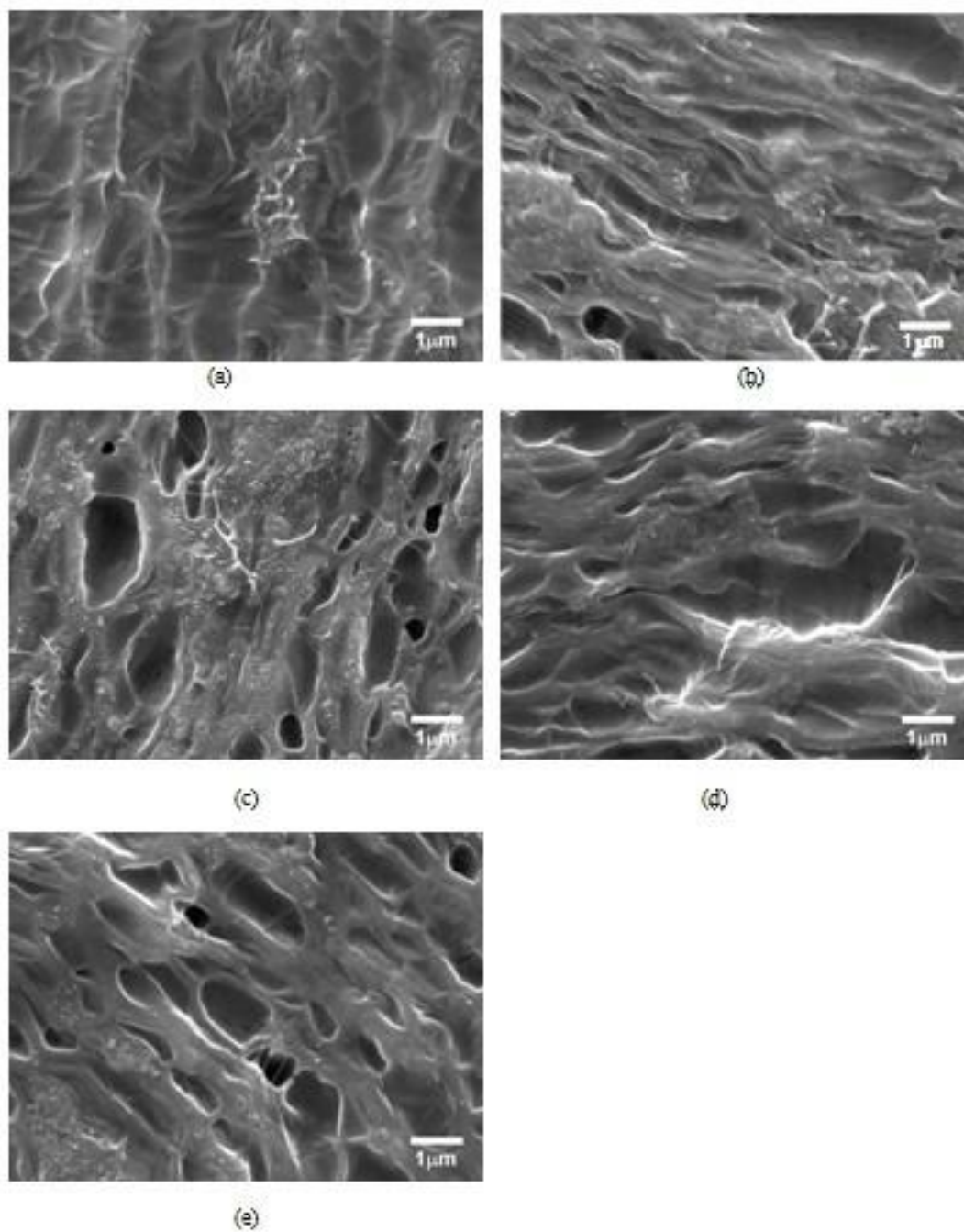


Fig. 3.11 SEM of composites dried at room temperature with 1:2 (a) and 1:4 (c) ratio of CNTs:PEDOT. Composites dried at 80°C with 1:2 (b) and 1:4 (d) ratio of CNTs:PEDOT. Composite with 1:4 ratio of CNTs:PEDOT initially dried at room temperature for 36 hours, then heated 80°C for 6 hours (e). The CNTs concentration for all composites is 9.8 wt%.

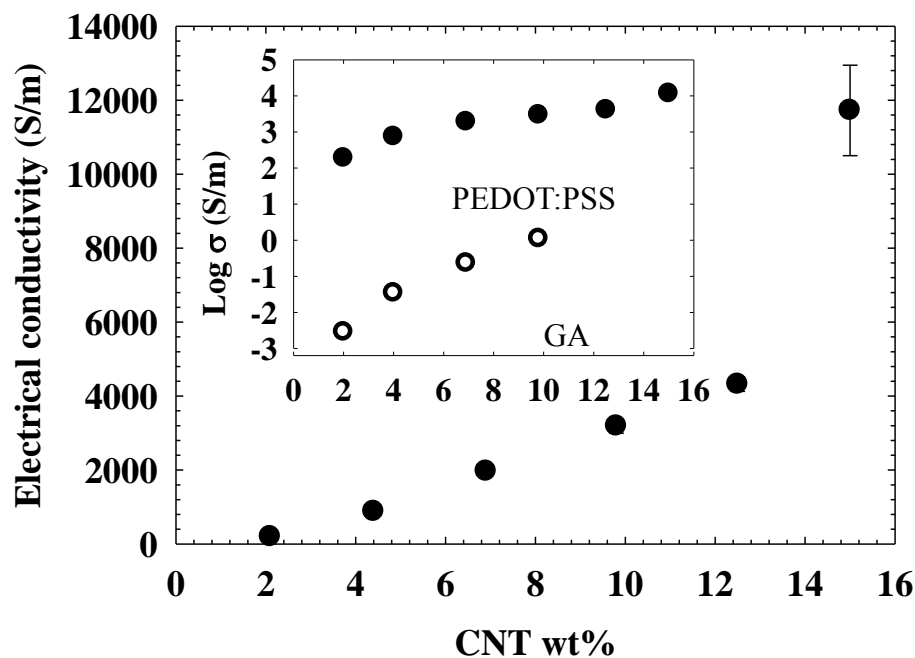


Fig. 3.12 Electrical conductivity of different CNTs concentration with CNTs:Stabilizer 1:4 ratio. The inset is a linear-log plot of the electrical conductivity as a function of the CNTs wt % with two different stabilizers, PEDOT:PSS and GA.

Figure 3.13 shows the thermopower of 2.1, 4.4, 6.9, 9.8, 12.5 and 15 wt % CNT composites with 1:4 ratio for CNTs and PEDOT:PSS at room temperature. In this composites, thermopower depends on PEDOT:PSS ($20\mu\text{V/K}$). When we synthesized a 30 wt% PEDOT:PSS(70 wt% airflex) composite without CNTs, the seebeck coefficient of the sample showed $17.6\mu\text{V/K}$ which was similar to the 1:4 ratio samples.

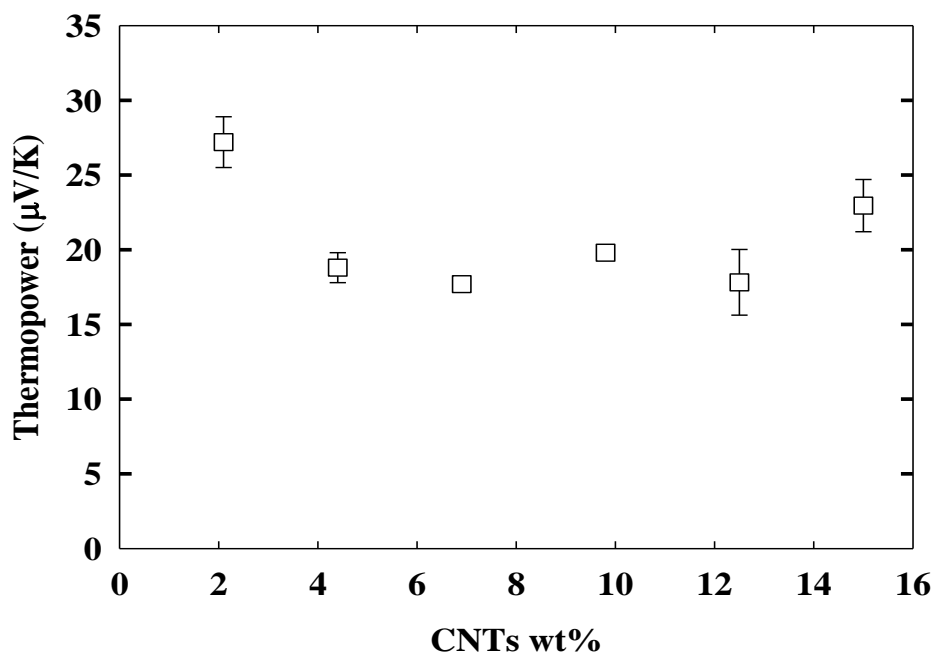


Fig. 3.13 Thermopower of different CNTs concentration with CNTs:PEDOT

Figure 3.14 shows the thermal conductivity of 2.1, 4.4, 6.9, 9.8, 12.5 and 15 wt % CNT composites with 1:4 ratio for CNTs and PEDOT:PSS at room temperature. As CNTs concentration increased, thermal conductivity also increased.

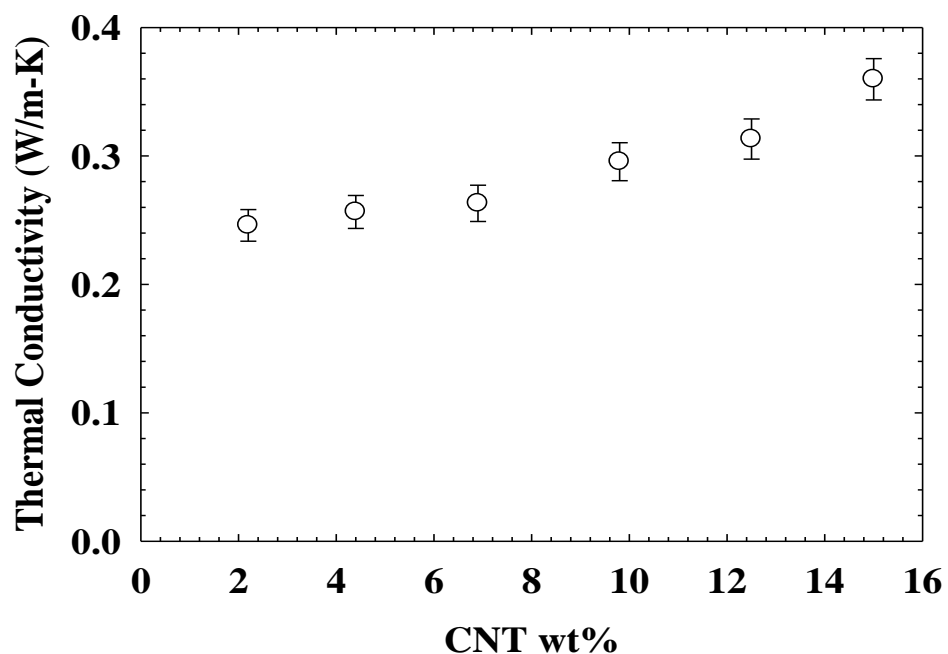


Fig. 3.14 Thermal conductivity of different CNTs concentration with CNTs:PEDOT

Figure 3.15 shows the electrical conductivities of the 1:1, 1:2, 1:3 and 1:4 CNTs/PEDOT:PSS ratio composites at room temperature and 80°C. In figure 3.15 and 3.16, as the PEDOT:PSS ratio increased, the electrical conductivity also increased up to the 1:4 ratio while the thermopower decreased. The seebeck coefficient of 1:1 ratio was dominated by CNTs and 1:4 ratio was dominated by PEDOT:PSS.

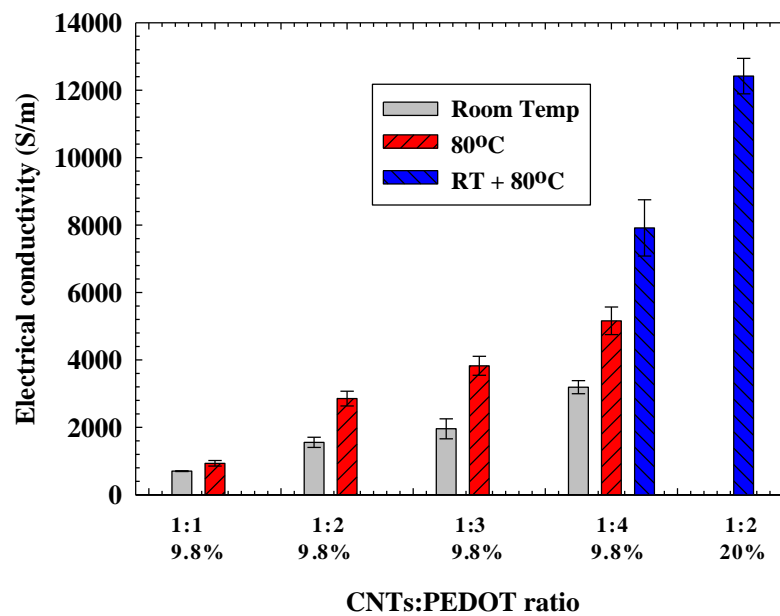


Fig. 3.15 Electrical conductivity of different ratio and drying condition (CNTs 9.8 wt%)

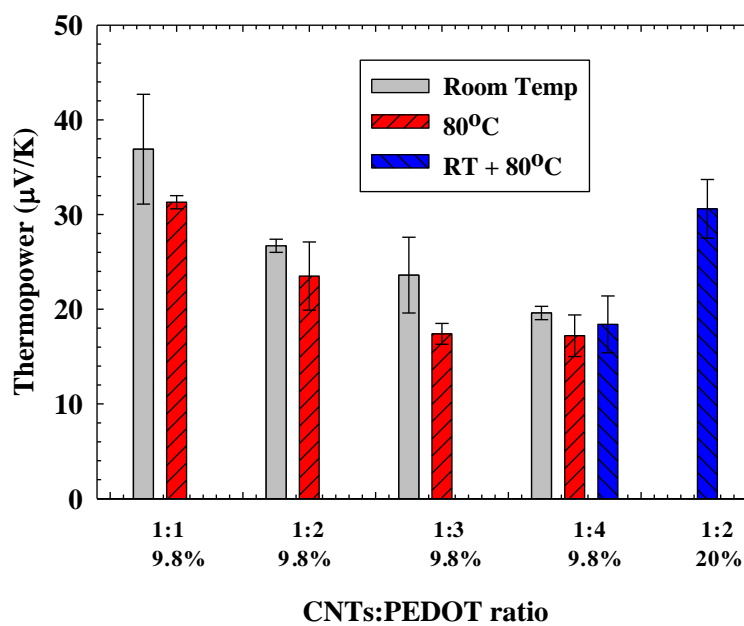


Fig. 3.16 Thermopower of different ratio and drying condition (CNTs 9.8 wt%)

The electrical conductivity increased as much as 1.5 ~ 2 times by changing drying temperature because drying under elevated temperature helps CNTs network to tighten and affects doping of PEDOT:PSS and DMSO. The composites dried at room temperature showed a significant level of porosity due to CNT aggregation. These pores are almost eliminated when the drying temperature was raised to 80°C due to the emulsion particles more effectively deforming around CNT particles and filling the gaps between them. As the drying temperature increases, the percolation threshold decreases due to the more rigid polymer particles forcing the CNTs into interstitial spaces more effectively, thereby forming the segregated network.³³

At 20 wt % CNTs with 1:2 ratio between CNTs and PEDOT:PSS which dried at room temperature and elevated temperature, electrical conductivity is 12,423 S/m. The percolation threshold was not further tested with very low CNT concentration, as the focus of this study was on high conductivity samples. Despite this large increase in electrical conductivity, thermopower was more or less constant (20 $\mu\text{V}/\text{K}$). This value is close to the thermopower of PEDOT:PSS as thermopower does not depend on filler dimensions and is strongly affected by more electrically conductive paths (composites have 4 times more PEDOT:PSS than CNTs). This feature is ideal for tailoring thermoelectric properties because the electrical conductivity can be increased without significantly sacrificing thermopower, which is opposite of the behavior observed in bulk crystalline materials. From the values of the thermoelectric parameters, ZT of the composite with 20 wt % CNTs was calculated to be ~ 0.01 at 300K, which is 10 times greater than that of previous studies with polymers and is close to typical semiconductor materials such as silicon ($ZT \sim 0.1$ at

300 K)⁷. Polymer nanocomposites could be economically viable even with a low ZT , considering the high power density (light-weight), low cost, simple manufacturing process, and non-toxicity. Fig. 3.17 shows the thermal conductivity of different CNTs:PEDOT ratio(CNTs 9.8 wt%). As CNTs and PEDOT ratio increased, thermal conductivity decreased. Figure 3.18, 3.19, 3.20 and 3.21 show the power factor ($S^2\sigma$) of CNTs and ZT values. In the figure 3.21, 0.01 of ZT value was achieved.

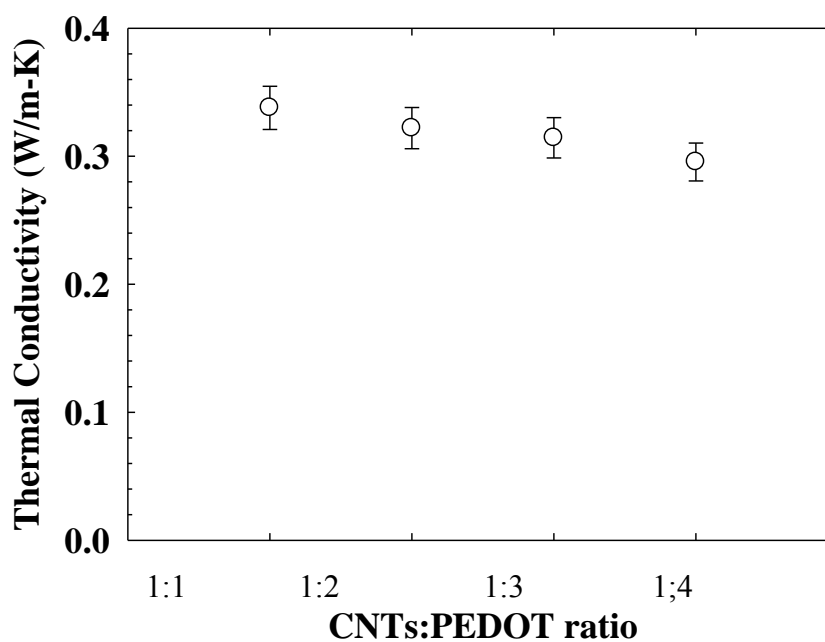


Fig. 3.17 Thermal conductivity of different CNTs:PEDOT ratio(CNTs 9.8 wt%)

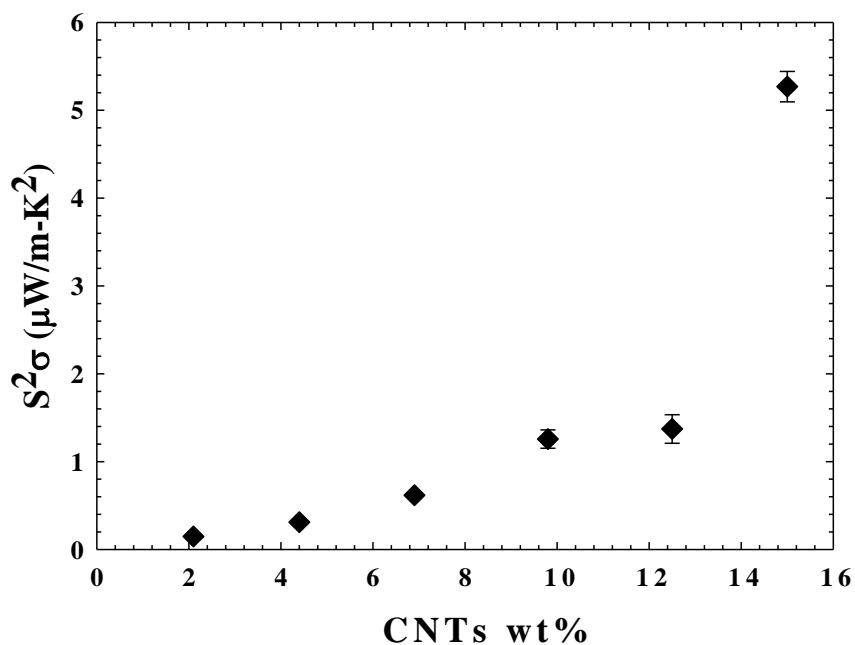


Fig. 3.18 Power factor ($S^2\sigma$) of CNTs concentration (1:4 ratio)

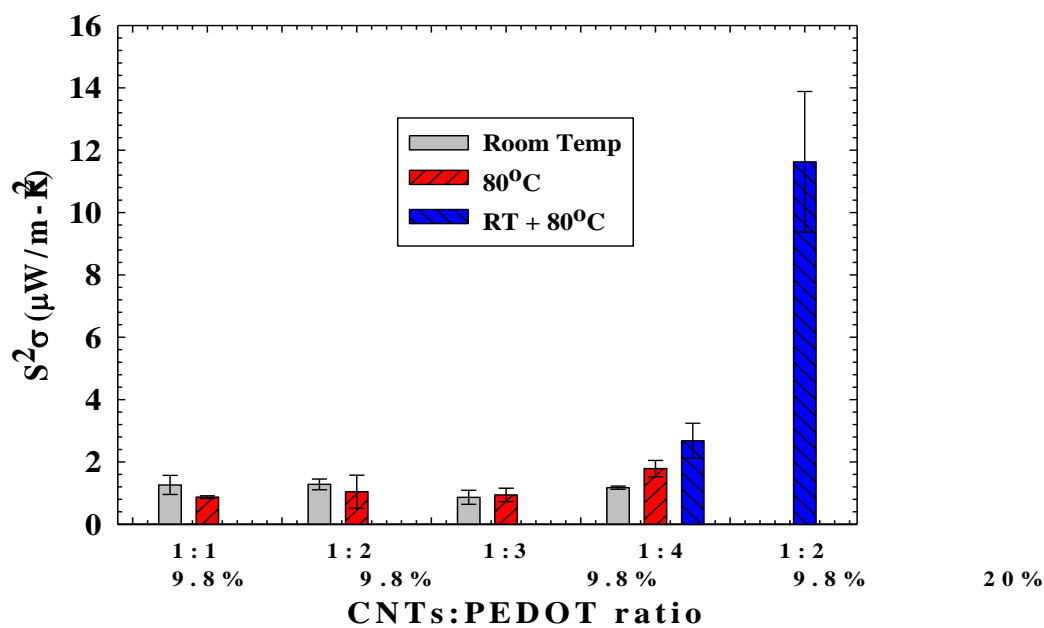


Fig. 3.19 Power factor ($S^2\sigma$) of different ratio and drying condition (CNTs 9.8 wt%)

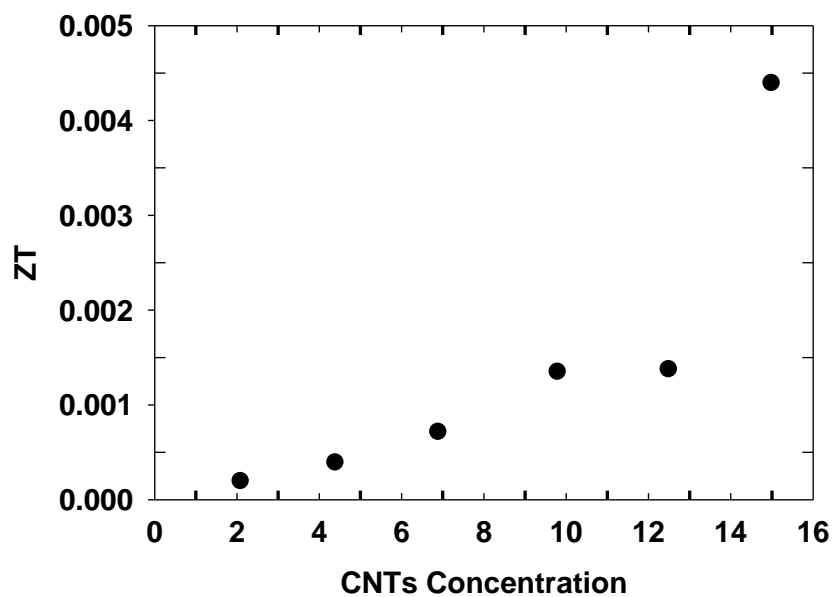


Fig. 3.20 ZT of CNTs concentration (1:4 ratio)

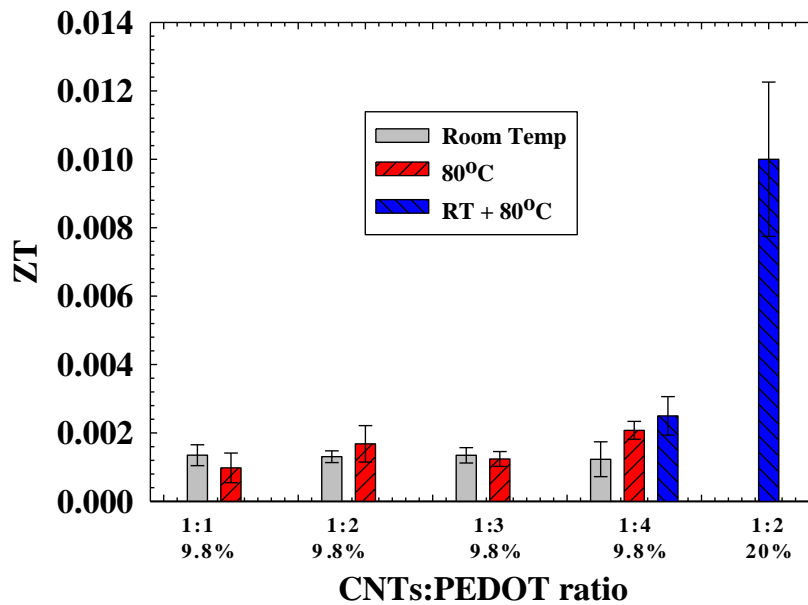


Fig. 3.21 ZT of different CNTs:PEDOT ratio (CNTs 9.8 wt%)

CHAPTER IV

CONCLUSION

Segregated-network CNT-polymer composites were prepared and their thermoelectric properties – thermal conductivity, electrical conductivity, and thermopower were measured as a function of CNT concentration at room temperature. This research demonstrates that the electrical conductivity of a polymer composite can be dramatically increased by incorporating CNTs in a segregated network fashion, while the thermal conductivity and thermopower were kept insensitive to the filler concentration. This behavior is believed to come from the thermally disconnected, but electrically connected, junctions that are present in the CNT networks which make it possible to tune the properties in favor of a higher thermoelectric figure of merit.

A series of segregated-network CNT-polymer composites with different stabilizer were also synthesized and their thermoelectric properties were measured as a function of CNT concentration. Composites with different ratios of CNTs and PEDOT:PSS at room temperature and elevated temperature were also measured. We show that for the effective dispersion of CNTs in water, the conductive polymer PEDOT:PSS can be used as a stabilizer at 1:4 ratio between CNTs and PEDOT:PSS. PEDOT:PSS is strongly absorbed to the CNT surface, the whole surface of CNTs can be covered by the PEDOT:PSS. The composite electrical conductivity could be related to the PEDOT:PSS. This study also demonstrates that the electrical conductivity of a polymer composite can be dramatically increased by incorporating CNTs, changing stabilizer and drying temperature. This was

done while the thermal conductivity and thermopower were kept insensitive to the filler concentration. Finally, it may be possible to achieve much greater improvement in the thermoelectric figure of merit for the polymer composite by using an intrinsically conductive polymer matrix and further varying filler materials and concentrations. Lightweight, low-cost, and non-toxic properties could make polymer composites economically viable even if their efficiency is less than that of current semiconductor materials.

REFERENCES

1. http://www.maxedoutmama.blogspot.com/2008_0701_archive.html
2. Chen, G.; Dresselhaus, M. S.; Dresselhaus, G.; Fleurial, J. P.; Caillat, T. Recent Developments in Thermoelectric Materials. *Int. Mater. Rev.* **2003**, *48*, (1), 45-66.
3. Tritt, T. M.; Boettner, H.; Chen, L. Thermoelectrics: Direct Solar Thermal Energy Conversion. *Mrs Bulletin* **2008**, *33*, (4), 366-368.
4. Heremans, J. P.; Jovovic, V.; Toberer, E. S.; Saramat, A.; Kurosaki, K.; Charoenphakdee, A.; Yamanaka, S.; Snyder, G. J. Enhancement of Thermoelectric Efficiency in PbTe by Distortion of the Electronic Density of States. *Science* **2008**, *321*, (5888), 554-557.
5. www.staff.aist.go.jp/english/nano-e.in.htm.
6. Winder, E. J.; Ellis, A. B. Thermoelectric Devices: Solid-State Refrigerators and Electrical Generators in the Classroom. *J. Chem. Edu.* **1996**, *73*, (10) 940-946.
7. Hostler, S.R.; Kaul, P.; Day, K.; Qu, V.; Cullen, C.; Abramson, A.R.; Xiaofeng Qiu; Burda, C. Thermal and Electrical Characterization of Nanocomposites for Thermoelectrics *IEEE conference*, **2006**, *1*, (1), 1-5.
8. Grunlan, J. C.; Kim, Y.-S.; Ziaee, S.; Wei, X.; Abdel-Magid, B.; Tao, K. Thermal and Mechanical Behavior of Carbon-Nanotube-Filled Latex. *Macromol. Mater. Eng.* **2006**, *291*, (9), 1035-1043.
9. Grunlan, J. C.; Gerberich, W. W.; Francis, L. F. Electrical and Mechanical Behavior of Carbon Black-Filled Poly(Vinyl Acetate) Latex-Based Composites. *Polym. Eng. Sci.* **2001**, *41*, (11), 1947-1962.
10. Grossiord, N.; Loos, J.; van, L.; Maryse, L.; Zakri, C.; John, H. A.; Koning, C. E.;

- Hart, J. High-Conductivity Polymer Nanocomposites Obtained by Tailoring the Characteristics of Carbon Nanotube Fillers. *Adv. Funct. Mater.* **2008**, *18*, (20), 3226-3234.
11. Yu, C.; Kim, Y. S.; Kim, D.; Grunlan, J. C. Thermoelectric Behavior of Segregated-Network Polymer Nanocomposites. *Nano Lett.* **2008**, *8*, (12), 4428-4432.
 12. Vaisman, L.; Wagner, H. D.; Marom, G. The Role of Surfactants in Dispersion of Carbon Nanotubes. *Adv. Colloid Interfac.* **2006**, *128*, (1), 37-46.
 13. Bandyopadhyaya, R.; Nativ-Roth, E.; Regev, O.; Yerushalmi-Rozen, R. Stabilization of Individual Carbon Nanotubes in Aqueous Solutions. *Nano Lett.* **2002**, *2*, (1), 25-28.
 14. Hobbie, E. K.; Obrzut, J.; Kharchenko, S. B.; Grulke, E. A. Charge Transport in Melt-Dispersed Carbon Nanotubes. *J. Chem. Phys.* **2006**, *125*, (4), 044712.
 15. Emmanuel, K.; Gehan, A. Electrical Properties of Single-Wall Carbon Nanotube-Polymer Composite Films. *J. Appl. Phys.* **2006**, *99*, (8), 084302.
 16. Marie, C. H.; Bert, K.; Andriy, V. K.; Paul, S.; Koning, C. E. Lowering the Percolation Threshold of Single-Walled Carbon Nanotubes Using Polystyrene/poly(3,4-ethylenedioxythiophene): Poly(styrene sulfonate) Blends. *Soft Matter* **2009**, *1*, (5), 878-885.
 17. Tummala, N. R.; Striolo, A. SDS Surfactants on Carbon Nanotubes: Aggregate Morphology. *ACS Nano*, **2009**, *3*, (3), 595-602.
 18. Kim, J. Y.; Jung, H. J.; Lee, D. E.; Joo, J. Enhancement of Electrical Conductivity of Poly(3,4-ethylenedioxythiophene)/Poly(4-styrenesulfonate) by a Change of Solvents. *Synthetic Metals* **2002**, *126*, 311-316.
 19. Joseph, L.; Grodzinski, J. Electronically Conductive Polymers. *Polym. Advan.*

- Technol.* **2002**, *13*, (9), 615-625.
20. Kirchmeyer, S.; Reuter, K. Scientific Importance, Properties and Growing Applications of Poly(3,4-ethylenedioxythiophene). *J. Mater Chem*, **2005**, *15*, (21), 2077-2088
 21. Groenendaal, L.; Jonas, F.; Freitag, D.; Pielartzik, H.; Reynolds, J. R. Poly(3,4-ethylenedioxythiophene) and Its Derivatives: Past, Present, and Future. *Adv. Mater.* **2000**, *12*, (7), 481-494.
 22. Ouyang, J.; Xu, Q.; Chu, C. W.; Yang Y.; Gang L.; Joseph S. On the Mechanism of Conductivity Enhancement in Poly(3,4-ethylenedioxythiophene):Poly(styrene sulfonate) Film Through Solvent Treatment. *Polymer* **2004**, *45*, 8443-8450.
 23. Ouyang, J.; Chu, C. W.; Chen, F. C.; Xu, Q.; Yang, Y. High-Conductivity Poly(3,4-ethylenedioxythiophene):Poly(styrene sulfonate) Film and Its Application in Polymer Optoelectronic Devices. *Adv. Funct. Mater.* **2005**, *15*, (2), 203-208.
 24. http://www.clevios.com/index.php?page_id=602
 25. De, S.; Lyons, P. E.; Sorel, S.; Doherty, E. M.; King, P. J.; Blau, W. J.; Nirmalraj, P. N.; Boland, J. J.; Scardaci, V.; Joimel, J.; Coleman, J. N. Transparent, Flexible, and Highly Conductive Thin Films Based on Polymer Nanotube Composites. *ACS Nano* **2009**, *3*, (3), 714-720.
 26. McCarthy, B.; Coleman, J. N.; Czerw, R.; Dalton, A. B.; Panhuis, M.; Maiti, A.; Drury, A.; Bernier, P.; Nagy, J. B.; Lahr, B.; Byrne, H. J.; Carroll, D. L.; Blau, W. J. A Microscopic and Spectroscopic Study of Interactions between Carbon Nanotubes and a Conjugated Polymer. *J. Phys. Chem. B* **2002**, *106*, (9), 2210-2216.
 27. O'Connell, M. J.; Boul, P.; Ericson, L. M. Reversible Water-Solubilization of Single-Walled Carbon Nanotubes by Polymer Wrapping *Chem. Phys. Lett.* **2001**, *342*, (4), 265-271.

28. Grunlan, J. C.; Mehrabi, A. R.; Bannon, M. V.; Bahr, J. L. Water-Based Single-Walled-Nanotube-Filled Polymer Composite with an Exceptionally Low Percolation Threshold. *Adv. Mater.* **2004**, *16*, (2), 150-153.
29. Hermant, M. C.; Klumperman, B.; Kyrylyuk, A. V.; Schoot, P. V.; Koning, C. E. Lowering the Percolation Threshold of Single-Walled Carbon Nanotubes Using Polystyrene/Poly(3,4-ethylenedioxythiophene): Poly(styrene sulfonate) Blends. *Soft Matter* **2009**, *5*, (4), 878-885.
30. Kirchmeyer, S.; Reuter, K. Scientific Importance, Properties and Growing Applications of Poly(3,4-ethylenedioxythiophene). *J. Mater. Chem* **2005**, *15*, (21), 2077-2088
31. Dawidczyk, T. J.; Walton, M. D.; Jang, W. S.; Grunlan, J. C. Layer-by-Layer Assembly of UV-Resistant Poly(3,4-ethylenedioxythiophene) Thin Films. *Langmuir* **2008**, *24*, (15), 8314-8318.
32. Kim, J. Y.; Jung, J. H.; Lee, D. E.; Joo, J. Enhancement of Electrical Conductivity of Poly(3,4-ethylenedioxythiophene)/Poly(4-styrenesulfonate) by a Change of Solvents. *Synthetic Met.* **2002**, *126*, (2-3), 311-316.
33. Kim, Y. W.; John, B.; Grunlan, J. C. Influence of Polymer Modulus on the Percolation Threshold of Latex-Based Composites. *Polymer* **2008**, *49*, (2), 570-578
34. Rutkofsky, M.; Banash, M.; Rajagopal, R.; Chen, J.; Corporation, Z. Using a Carbon Nanotube Additive to Make Electrically Conductive Commercial Polymer Composites. *ZYVEX* **2006**, *1*, (1), 1-5
35. Yu, C.; Shi, L.; Yao, Z.; Li, D.; Majumdar, A. Thermal Conductance and Thermopower of an Individual Single-Wall Carbon Nanotube. *Nano Lett.* **2005**, *5*, (9), 1842-1846.

36. Shi, L.; Li, D.; Yu, C.; Jang, W. Y.; Kim, D.; Yao, Z.; Kim, P.; Majumdar, A. Measuring Thermal and Thermoelectric Properties of One-Dimensional Nanostructures Using a Microfabricated Device. *J. Heat Transfer* **2003**, *125*, 881-888.
37. Hone, J.; Llaguno, M. C.; Nemes, N. M.; Johnson, A. T.; Fischer, J. E.; Walters, D. A.; Casavant, M. J.; Schmidt, J.; Smalley, R. E. Electrical and Thermal Transport Properties of Magnetically Aligned Single Wall Carbon Nanotube Films. *Appl. Phys. Lett.* **2000**, *77*, (5), 666-668.
38. Hone, J.; Llaguno, M. C.; Biercuk, M. J.; Johnson, A. T.; Batlogg, B.; Benes, Z.; Fischer, J. E. Thermal Properties of Carbon Nanotubes and Nanotube-Based Materials *Appl. Phys. A* **2002**, *74*, 339-343.
39. Hone, J.; Whitney, M.; Piskoti, C.; Zettl, A. Thermal Conductivity of Single-Walled Carbon Nanotubes. *Phys. Rev. B* **1999**, *59*, (4). 2514-2516
40. Berber, S.; Kwon, Y. K.; Tománek, D. Unusually High Thermal Conductivity of Carbon Nanotubes. *Phys. Rev. Lett.* **2000**, *84*, (20), 4613 - 4616.
41. Ce-Wen, N.; Gang, L.; Yuanhua, L.; Ming, L. Interface Effect on Thermal Conductivity of Carbon Nanotube Composites. *Appl. Phys. Lett.* **2004**, *85*, (16), 3549-3551.
42. Huxtable, S. T.; Cahill, D. G.; Shenogin, S.; Xue, L.; Ozisik, R.; Barone, P.; Usrey, M.; Strano, M. S.; Siddons, G.; Shim, M.; Keblinski, P. Interfacial Heat Flow in Carbon Nanotube Suspensions. *Nature Materials* **2003**, *2*, 731 - 734.

VITA

Dasaroyong Kim was born in 1981 in Jeomchon, The Republic of Korea. He received a B.S. in Weapon's Engineering from the Korea Military Academy in 2004. He was then commissioned as an Infantry officer. He served in the ROK Army from 2004 to 2007 as a platoon leader and aide-de-camp to commander. He entered the Mechanical Engineering Department at Texas A&M University in 2007 as an M.S. student and graduated in August 2009.

Permanent Address: Department of Mechanical Engineering, 3123, TAMU,
College Station, Texas, 77843-3123, USA.

Chair of Committee: Dr. Choongho Yu

E-mail Address: 64dakkang@gmail.com